

# Radiation-resistant metal-organic framework enables efficient separation of krypton fission gas from spent nuclear fuel

Sameh K. Elsaidi <sup>1,2,3✉</sup>, Mona H. Mohamed<sup>4,5</sup>, Ahmed S. Helal<sup>6,7</sup>, Mitchell Galanek<sup>8</sup>, Tony Pham <sup>9,10</sup>, Shanelle Suepaul<sup>10</sup>, Brian Space <sup>10</sup>, David Hopkinson<sup>3</sup>, Praveen K. Thallapally<sup>11✉</sup> & Ju Li <sup>7✉</sup>

Capture and storage of volatile radionuclides that result from processing of used nuclear fuel is a major challenge. Solid adsorbents, in particular ultra-microporous metal-organic frameworks, could be effective in capturing these volatile radionuclides, including <sup>85</sup>Kr. However, metal-organic frameworks are found to have higher affinity for xenon than for krypton, and have comparable affinity for Kr and N<sub>2</sub>. Also, the adsorbent needs to have high radiation stability. To address these challenges, here we evaluate a series of ultra-microporous metal-organic frameworks, SIFSIX-3-M (M = Zn, Cu, Ni, Co, or Fe) for their capability in <sup>85</sup>Kr separation and storage using a two-bed breakthrough method. These materials were found to have higher Kr/N<sub>2</sub> selectivity than current benchmark materials, which leads to a notable decrease in the nuclear waste volume. The materials were systematically studied for gamma and beta irradiation stability, and SIFSIX-3-Cu is found to be the most radiation resistant.

<sup>1</sup> Department of Chemical and Biomolecular Engineering, University of California, Berkeley, Berkeley, CA 94720, USA. <sup>2</sup> Oak Ridge Institute for Science and Education, Pittsburgh, PA 15236, USA. <sup>3</sup> DOE National Energy and Technology Laboratory (NETL), Pittsburgh, PA 15236, USA. <sup>4</sup> Department of Chemistry, University of Pittsburgh, 219 Parkman Avenue, Pittsburgh, USA. <sup>5</sup> Chemistry Department, Faculty of Science, Alexandria University, P.O. Box 426, Ibrahimia, Alexandria 21321, Egypt. <sup>6</sup> Nuclear Materials Authority, P.O. Box 540, El Maadi, Cairo, Egypt. <sup>7</sup> Department of Nuclear Science and Engineering and Department of Materials Science and Engineering, Massachusetts Institute of Technology, Cambridge, MA 02139, USA. <sup>8</sup> Office of Environment, Health & Safety, Massachusetts Institute of Technology, Cambridge, MA 02139, USA. <sup>9</sup> Department of Chemistry, Biochemistry, and Physics, The University of Tampa, 401 West Kennedy Boulevard, Tampa, FL 33606-1490, USA. <sup>10</sup> Department of Chemistry, University of South Florida, 4202 East Fowler Avenue, CHE205, Tampa, FL 33620, USA. <sup>11</sup> Physical and Computational Science Directorate, Pacific Northwest National Laboratory, Richland, WA 99352, USA. ✉email: [samehelsaidi@mail.usf.edu](mailto:samehelsaidi@mail.usf.edu); [Praveen.thallapally@pnnl.gov](mailto:Praveen.thallapally@pnnl.gov); [liju@mit.edu](mailto:liju@mit.edu)

Nuclear energy is an emission free, high-energy density source with minimal land use. However, any future expansion of civilian nuclear power will most likely require efficient management of used nuclear fuel (UNF). UNF processing minimizes radioactive waste, but the release of volatile radionuclides is a significant challenge. The nature of the volatile radionuclides depends on the reprocessing procedure and generally consists of a mixture of noble gases (predominantly  $^{85}\text{Kr}$ , which  $\beta$  or  $\beta\gamma$  decays to stable  $^{85}\text{Rb}$  with  $t_{1/2} = 10.8$  years, along with Xe), and species containing  $^{129}\text{I}$ <sup>1–5</sup>. The current reprocessing technologies can capture other volatile radionuclides with relative ease, but an efficient system to capture (and store)  $^{85}\text{Kr}$  needs to be in place. While methods such as cryogenic distillation and fluorocarbon based absorption have been proposed and tested, they are expensive and require complex engineering control. Solid-state adsorbents, in particular porous metal-organic frameworks (MOFs), could be better alternatives to capture these volatile radionuclides including  $^{85}\text{Kr}$ .

Physisorption-based adsorption and storage is deemed an energy-efficient process that can be operated at near-ambient conditions and is easier to integrate into current engineering setups. Several traditional adsorbents such as zeolites and activated carbon have been tested, but were found to have low capacity and selectivity (over Xe and other competing gases). MOFs are known for their versatile architecture and functionalized pore surface and have shown promise for gas sorption and separation<sup>1,6–16</sup>. However, as Xe is considerably more polarizable than Kr, porous materials such as MOFs are generally more selective toward Xe over Kr due to stronger van der Waals interactions, which causes further engineering challenges as the Xe will lead to reduced Kr adsorption<sup>2,7,15,17–19</sup>. To avoid this, we recently reported a proof-of-concept study where a dual-bed system, fitted in series, was utilized to separate and store Kr<sup>20</sup>. The gas stream (known as off-gas, 400 ppm of Xe and 40 ppm of Kr mixed with air, which are the typical concentrations of the off-gas in a reprocessing plant) is first directed through a Xe selective adsorbent bed to remove the Xe, followed by removal of Kr in the second bed using the same or another adsorbent material. In the absence of the competing Xe in the second bed, the adsorbent is expected to have enhanced Kr storage capacity, even when using identical adsorbent material (which is the modality used in this paper). The enhancement and the total Kr uptake depend on the selectivity for Kr over competing gases (e.g.,  $\text{N}_2$ ,  $\text{O}_2$ ). The stored gas in the second bed has a high Kr, low Xe feature, so the second bed can be fluidized and/or regenerated (with temperature controlled desorption) with such characteristics in mind. The MOFs in both the first bed and the second bed should be sufficiently radiation resistant to beta and gamma radiations as  $^{85}\text{Kr}$  flows pass or stores in them. Only a few MOFs have been studied for their radiation stability<sup>20,21</sup>. Lee et al. reported the potential of three MOFs (MIL-100(Fe), MIL-101(Cr), and UiO-66(Zr)) for Xe/Kr separation<sup>22</sup>. The study showed that UiO-66(Zr) is the most promising adsorbent among the three candidates; however, the radiation stability of UiO-66(Zr) has been performed under low radiation dose of only 2 kGy which is not relevant to the practical Xe/Kr separation at nuclear reprocessing plants.

In our continuous search for materials with high Kr adsorption capacity and selectivity, we synthesized, measured and analyzed the SIFSIX-3-M series (M = Zn, Cu, Ni, Co, Fe) of MOFs<sup>7,23–25</sup>. SIFSIX-3-M is a class of isorecticular hybrid ultra-microporous materials (HUMs) based on saturated metal centers (SMCs) and  $\text{SiF}_6^{-2}$  pillars<sup>26,27</sup>. SIFSIX-3-M can be tuned for Kr separation by substituting different metal centers including  $\text{Zn}$ <sup>27,28</sup>,  $\text{Co}$ <sup>29</sup>,  $\text{Cu}$ <sup>30</sup>,  $\text{Ni}$ <sup>29</sup>, or  $\text{Fe}$ <sup>8</sup>. SIFSIX-3-M materials are known for their very low affinity toward  $\text{N}_2$  and for exceptional performance in selectively removing  $\text{CO}_2$  from air, which makes them great candidates for

two-bed breakthrough setup. In this study, two columns were filled by adsorbent material that has a preferential adsorption of gases  $\text{Xe}$ ,  $\text{CO}_2 > \text{Kr} > \text{N}_2$  and  $\text{O}_2$ . The Xe and  $\text{CO}_2$  gases will be selectively adsorbed over the rest of gases in the first bed while the Kr will be preferentially adsorbed over the  $\text{N}_2$  and  $\text{O}_2$  in the second bed. The advantage of this method is that we can separate the radioactive  $^{85}\text{Kr}$  into a high purity gas. The presence of other gases mixed with  $^{85}\text{Kr}$  would otherwise increase the waste volume to be disposed and therefore increase the cost of the UNF reprocessing (Fig. 1).

## Results

**Radiation stability study.** The MOF materials were exposed to gamma radiation ( $^{60}\text{Co}$  source) from 0 to 200 kGy and the stability of the materials was monitored by powder X-ray diffraction (PXRD) to confirm the retention of their crystallinity after  $\gamma$  irradiation (see Methods section for experimental details) and  $\beta$  irradiation. The near equivalence in radiation damage tolerance dose between  $^{85}\text{Kr}$   $\beta$  and  $^{60}\text{Co}$   $\gamma$ -rays was well established, for example “no significant difference in the decomposition yield was observed” in fluorocarbons exposed to beta and gamma radiation of the same dose<sup>31</sup>.

Quantitative analyses of the PXRD data using the Rietveld and Pawley fitting methods were performed to compare the as-synthesized structures with the irradiated structures (Supplementary Figs. 3–17). As shown in Figs. 2 and 3 and Supplementary Figs. 3 and 4, the Zn and Ni analogs are unstable and show phase change at 1 kGy. SIFSIX-3-Fe maintained its crystallinity at 1 kGy. Further irradiation of SIFSIX-3-Fe to 3 and 10 kGy leads to new unknown phases as shown in Supplementary Figs. 4–8. The new phase is a mixture of a 1D structure with water coordinated to Fe (Fig. 2) and another unknown phase. The original structure of SIFSIX-3-Fe is strongly distorted and almost vanished. The SIFSIX-3-Co structure was stable up to 10 kGy before it undergoes phase change (Supplementary Figs. 9–12). From the PXRD pattern of irradiated MOF at 3 kGy, higher peak intensity for the (110) peak at  $17.65^\circ$  was observed which may be attributed to spinning of fluorine atoms into the (110) plane (Supplementary Fig. 11). Based on these results the crystal structure of SIFSIX-3-Co remains unaltered under 3 kGy radiation. After 10 kGy radiation, the crystal structure is altered and presents the original SIFSIX-3-Co structure as well as another unknown phase. The unit cell and space group are determined from the unknown phase peak positions (Supplementary Fig. 12) to be tetragonal (4/m) with lattice parameters  $a = 16.086 \text{ \AA}$  and  $c = 12.952 \text{ \AA}$ , which does not exist in the CCDC database<sup>32</sup>.

SIFSIX-3-Cu was the most stable MOF (Supplementary Figs. 13–17) and it maintained its crystallinity up to 50 kGy  $\gamma$  irradiation. According to Cambridge Structural Database (CSD)<sup>33</sup>, Cu tends to bond with N donor ligand more readily compared with Co, Fe, Zn, and Ni. The Cu–N bonds are stronger than those of other M–N analogs. This is supported by shorter Cu–N bond distance of 1.9  $\text{Å}$  in the SIFSIX-3-Cu compared with the other the M–N analogs (2.1  $\text{Å}$ ). Also, it was reported that the SIFSIX-3-Cu has a slightly smaller unit cell of  $378 \text{ \AA}^3$  versus  $388 \text{ \AA}^3$  (SIFSIX-3-Zn), where the authors attributed this observation to the relatively stronger bonding between the Cu(II) and the pyrazine<sup>30</sup>. Therefore, M–N bond strength could be the main factor behind the stability of SIFSIX-3-Cu framework which reaches up to 50 kGy, while other materials demonstrate much lower stability that reaches to maximum 10 kGy (in case of Co). For this class of the isorecticular SIFSIX-3-M structures, it was reported that the change in metal center or the environment around it could lead to different properties of the MOF material<sup>8,21,29,30,34</sup>.

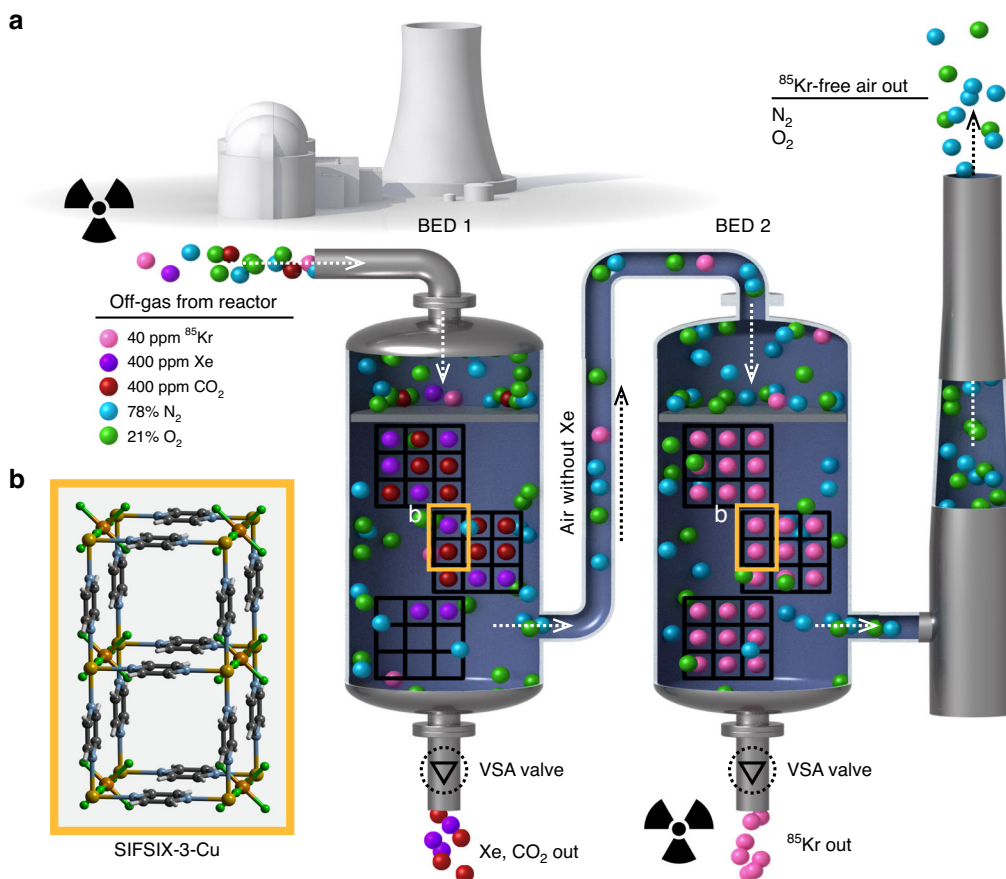


**Fig. 1 Schematic representation of the two-bed breakthrough setup.** **a** Illustration of the two-bed technique for removal of radioactive Kr from nuclear reprocessing plants using SIFSIX-3-Cu. **b** Each two squares in the bed 1 and bed 2 represent two channels of SIFSIX-3-Cu structure. Atom colors: C = gray, H = white, N = light blue, F = green, Si = light brown, Cu = orange, O = red, Xe = violet, Kr = pink.

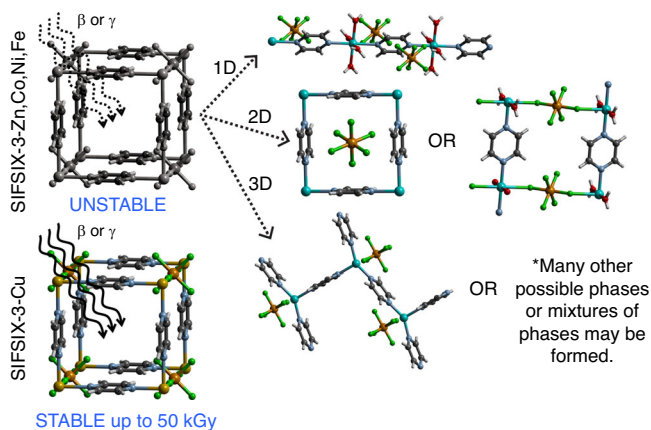


**Fig. 2 Illustration of impact of irradiation on SIFSIX-3-M materials.** The SIFSIX-3-M (M = Zn, Co, Ni, Fe) structures decompose to 1D, 2D or many other possible phases up on radiation exposure. The SIFSIX-3-Cu is stable and maintains its original crystal structure up to 50 kGy dose in beta or gamma radiation. Atom colors: C = gray, H = white, N = light blue, F = green, Si = light brown, Cu = orange, M (Ni, Co, Fe, Zn) = cyan, O = red.

The beta radiation stability of the SIFSIX-3-Cu was evaluated by irradiating the activated sample with 1.5 MeV electrons beam at a dose rate of 50 kGy/h and comparing its PXRD pattern with the simulated SIFSIX-3-Cu pattern. Figure 3f showed that the activated SIFSIX-3-Cu sample is stable after 50 kGy beta

irradiation. <sup>85</sup>Kr concentration is reported to be 1130–1800 TBq/Mg (3510–48,600 Ci/Mg) of spent fuel<sup>35</sup>. Based on these concentrations, the radiation dose rate to 1 g SIFSIX-3-Cu from absorbing all the <sup>85</sup>Kr in 1 g of spent nuclear fuel was calculated (see Supplementary Note 3). According to the obtained results from both beta and gamma irradiation experiments, SIFSIX-3-Cu is radiation resistant up to 50 kGy. Hence, 1 g of SIFSIX-3-Cu can separate <sup>85</sup>Kr effectively from 2674 g of spent nuclear fuel (130 TBq/Mg case) or 188 g spent nuclear fuel (1800 TBq/Mg case), without any crystal structure damage, if keeping all the <sup>85</sup>Kr inside for 1 h.

**Single-component gas adsorption study.** The single-component CO<sub>2</sub>, Xe, Kr, N<sub>2</sub>, and O<sub>2</sub> adsorption isotherms of SIFSIX-3-Cu at 298 K (Fig. 4a) showed a preferential adsorption of CO<sub>2</sub> and Xe over Kr which will allow CO<sub>2</sub> and Xe capture in the first bed, and a high Kr/N<sub>2</sub> selectivity which facilitates the capture of the <sup>85</sup>Kr in the second bed.

**Modeling study.** As revealed through modeling studies, the larger atomic radius of Xe provided for a better fit within the square pores as well as the region enclosed by four neighboring SiF<sub>6</sub><sup>2-</sup> pillars in the material (Fig. 4b, c and Supplementary Figs. 23 and 24). Furthermore, density functional theory (DFT) calculations confirm that SIFSIX-3-Cu is selective for CO<sub>2</sub> and Xe over Kr, and Kr over N<sub>2</sub> and O<sub>2</sub> on the basis of the DFT calculated adsorption energies in the material (see Supplementary Note 5 and Supplementary Table 1).

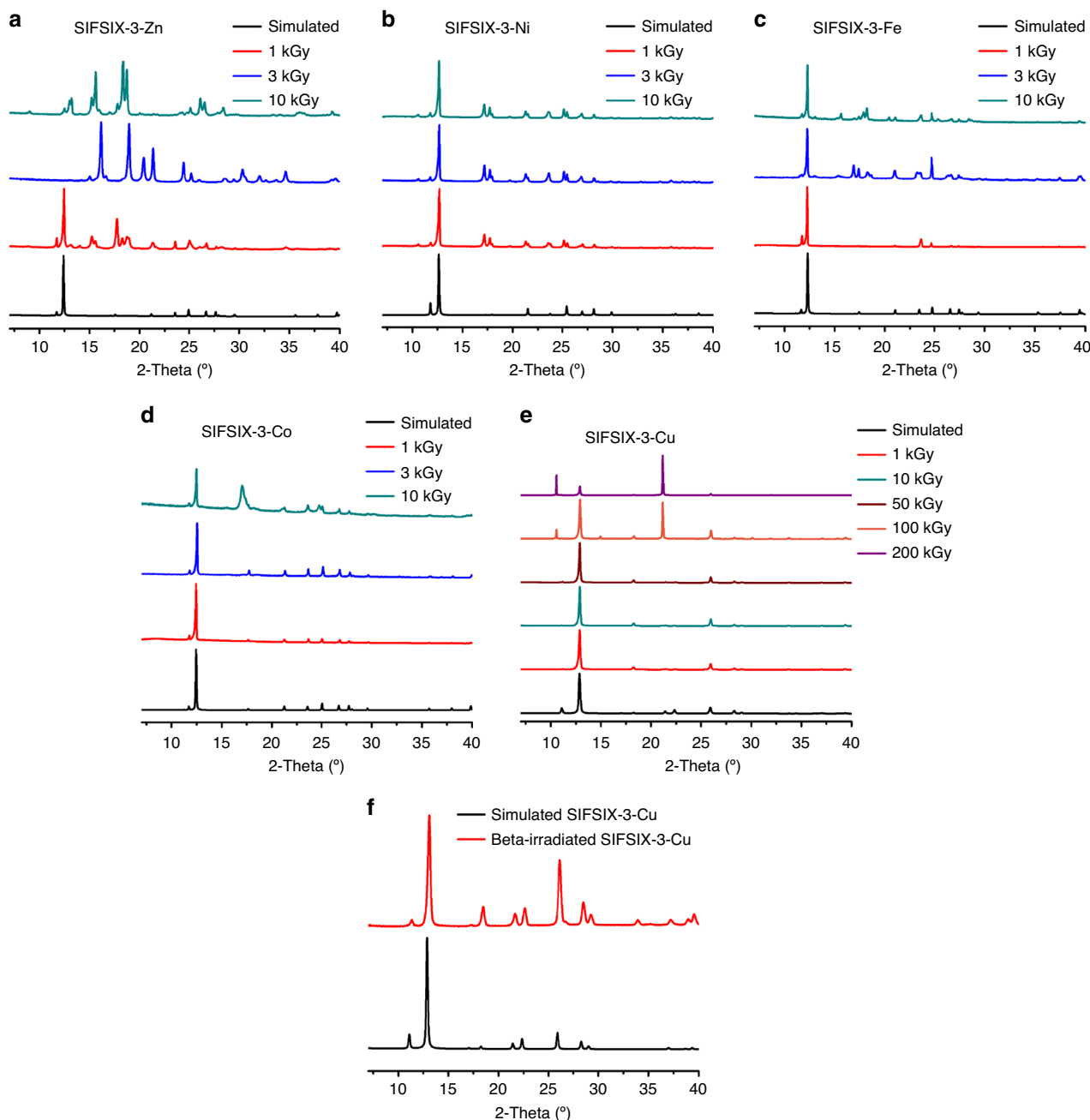


**Fig. 3** Powder X-ray diffraction patterns of irradiated and simulated SIFSIX-3-M structures. **a** gamma-irradiated SIFSIX-3-Zn, **b** gamma-irradiated SIFSIX-3-Ni, **c** gamma-irradiated SIFSIX-3-Fe, **d** gamma-irradiated SIFSIX-3-Co, and **e** SIFSIX-3-Cu and **f** activated SIFSIX-3-Cu structure after 50 kGy beta irradiation.

**Two-bed breakthrough adsorption study.** We ran the two-bed breakthrough experiments, where both beds use SIFSIX-3-Cu, because of its high radiation stability (Fig. 3e). First, a single-bed test was performed on SIFSIX-3-Cu (Fig. 5a, b) in order to show the ability of SIFSIX-3-Cu for separation of Kr gas from N<sub>2</sub> and O<sub>2</sub>. Second, single-bed experiments were run for the simulated off-gas containing 400 ppm Xe and 40 ppm Kr balanced with dry air, revealing the time needed for each gas to break through from the first bed under the conditions of simulated off-gas stream. Accordingly, this information informed us of when to switch on the second bed in the two-bed system before Xe and CO<sub>2</sub> start to break through (see Fig. 1, Supplementary Note 6 and Supplementary Scheme 1). The single-bed breakthrough experiments for 1000 ppm Kr balanced with dry air revealed that SIFSIX-3-Cu can

selectively adsorb Kr over N<sub>2</sub> and O<sub>2</sub> as shown in Fig. 5 and Table 1.

Based on the single-column experiment, SIFSIX-3-Cu can selectively separate Xe from gas mixture 1 consisting of 400 ppm Xe, 40 ppm Kr balanced with dry air. The column breakthrough experiment suggests that Xe breakthrough occurs at  $t_1^{\text{finish}} = 29$  min, thus by connecting a second bed loaded with adsorbent material before this time, we will be able to capture the Kr in the second bed before the Xe breaks through the first bed (see Fig. 5). We note that  $t_1^{\text{finish}}$  certainly depends on the size and geometric design of the first bed (which can be fluidized<sup>36</sup>), i.e., it is not just a material property.

The two-column breakthrough system consists of two adsorption beds in series that were packed with 1 g of SIFSIX-3-Cu in

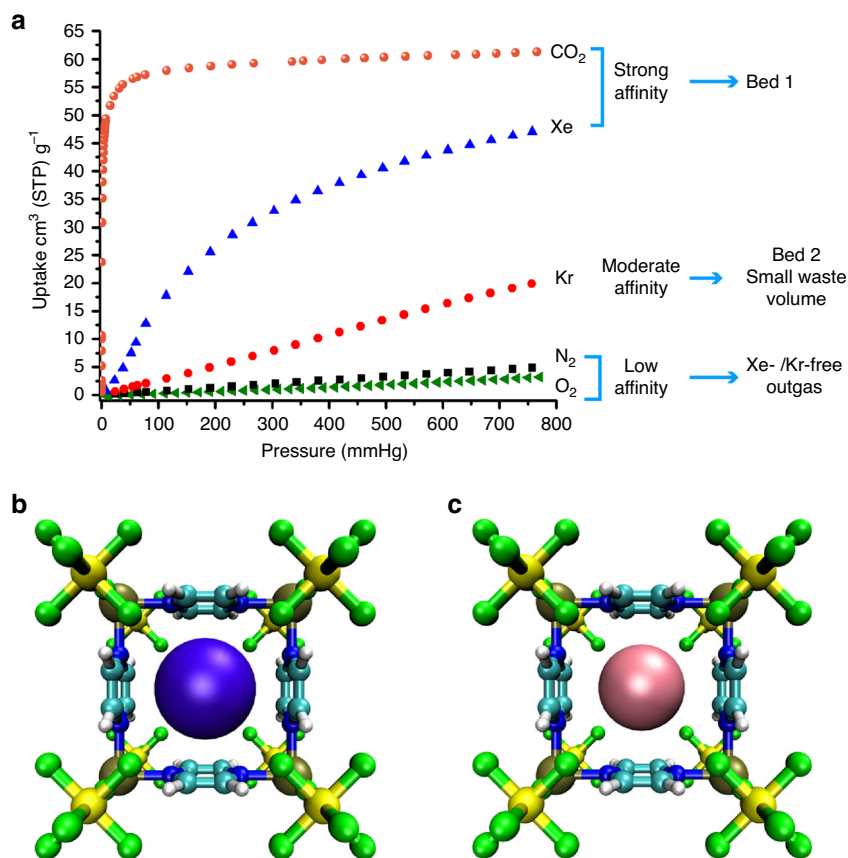


**Fig. 4** Gas adsorption properties and binding sites. **a** Single-component CO<sub>2</sub>, Xe, Kr, N<sub>2</sub>, and O<sub>2</sub> adsorption isotherms at 298 K for SIFSIX-3-Cu. Molecular illustration of the most favorable binding site for **b** Xe and **c** Kr in SIFSIX-3-Cu (top view) as determined from simulated annealing calculations. Atom colors: C = cyan, H = white, N = blue, F = green, Si = yellow, Cu = gold, Xe = violet, Kr = pink.

each bed. The adsorbent beds were purged with He and then a gas mixture containing 400 ppm Xe and 40 ppm Kr balanced with dry air at a total pressure of 1 bar was introduced to the first bed (with the second bed bypassed). Breakthrough curves indicate that the Xe gas and CO<sub>2</sub> were retained by the first bed, leaving 40 ppm Kr balanced with dry air at the outlet. At time  $t_2^{\text{start}} = 18$  min, the second bed was enabled, thus flowing gas from the first bed to the second. Gas analysis shows that Kr concentration drops as it is adsorbed into the second bed, and fully breaks through again at  $t_2^{\text{finish}} =$  around 30 min. In practice the feed gas would be directed to a new bed, while the Kr loaded bed is regenerated. It is important to note that the adsorbent material can capture Kr gas over the competing gases that could increase the waste volume. The benchmark materials, SBMOF-1<sup>37</sup>, Ni-MOF-74<sup>38</sup>, and Ag mordenite<sup>39</sup>, showed remarkable performance for Xe/Kr separation, however, they are not suitable for <sup>85</sup>Kr separation from spent fuel using the two-bed technique. Ni-MOF-74<sup>38</sup> and Ag mordenite<sup>39</sup> were found to have poor Kr/N<sub>2</sub> selectivity (Supplementary Figs. 21 and 30), while, SBMOF-1<sup>37</sup> showed low Kr/CO<sub>2</sub> which prohibit the separation of the Kr in pure form (Supplementary Fig. 22).

As shown in Fig. 5 and Table 1, SIFSIX-3-Cu showed a great potential for Kr removal from simulated UNF off-gas using the two-bed system. The calculated capacity of the adsorbed Xe in first bed by SIFSIX-3-Cu at equilibrium was found to be 6.74 mmol/kg while the capacity of the Kr captured in second bed is 0.15 mmol/kg. This system is a feasible and efficient way to separate and capture Xe and Kr at ambient conditions. This further demonstrates that once the competing gas, Xe, is removed in the first bed using SIFSIX-3-Cu, the Kr removal efficiency was

increased significantly, which can lead to a notable decrease in the waste volume at the UNF reprocessing plant.

## Discussion

In summary, we evaluated the performance of a family of ultra-microporous pillared square lattices, SIFSIX-3-M (M = Fe, Co, Ni, Cu, Zn) for <sup>85</sup>Kr removal from used nuclear fuel. The radiation stability was examined by exposing the materials to varying levels of gamma radiation and beta radiation.

SIFSIX-3-Cu is the only material in this family suitable for this application based on radiation stability up to 50 kGy for both beta and gamma radiations.

The choice of the right material for the <sup>85</sup>Kr separation from nuclear reprocessing plants is based on several criteria: (1) Preferential adsorption of Xe and CO<sub>2</sub> over Kr so these two gases can be separated in the first bed, and (2) Preferential adsorption of Kr over N<sub>2</sub> and O<sub>2</sub> so that Kr can be adsorbed in the second bed in more pure form with minimum waste volume. If the material fulfills these two criteria, then it should be qualified for the radiation stability. If the material does not achieve these two criteria, it is not helpful in this context to examine their radiation stability because they did not fulfill the main purpose of the Kr removal presented herein, which is the reduction of waste volume and Kr separation in more pure form with minimal amounts of other competing gases.

The single-component adsorption isotherms revealed that SIFSIX-3-Cu can preferentially adsorb CO<sub>2</sub> and Xe over Kr, and Kr over N<sub>2</sub> and O<sub>2</sub>; these findings have been supported by modeling. The practical use of SIFSIX-3-Cu in Kr capture and separation from nuclear fuel reprocessing off-gas was

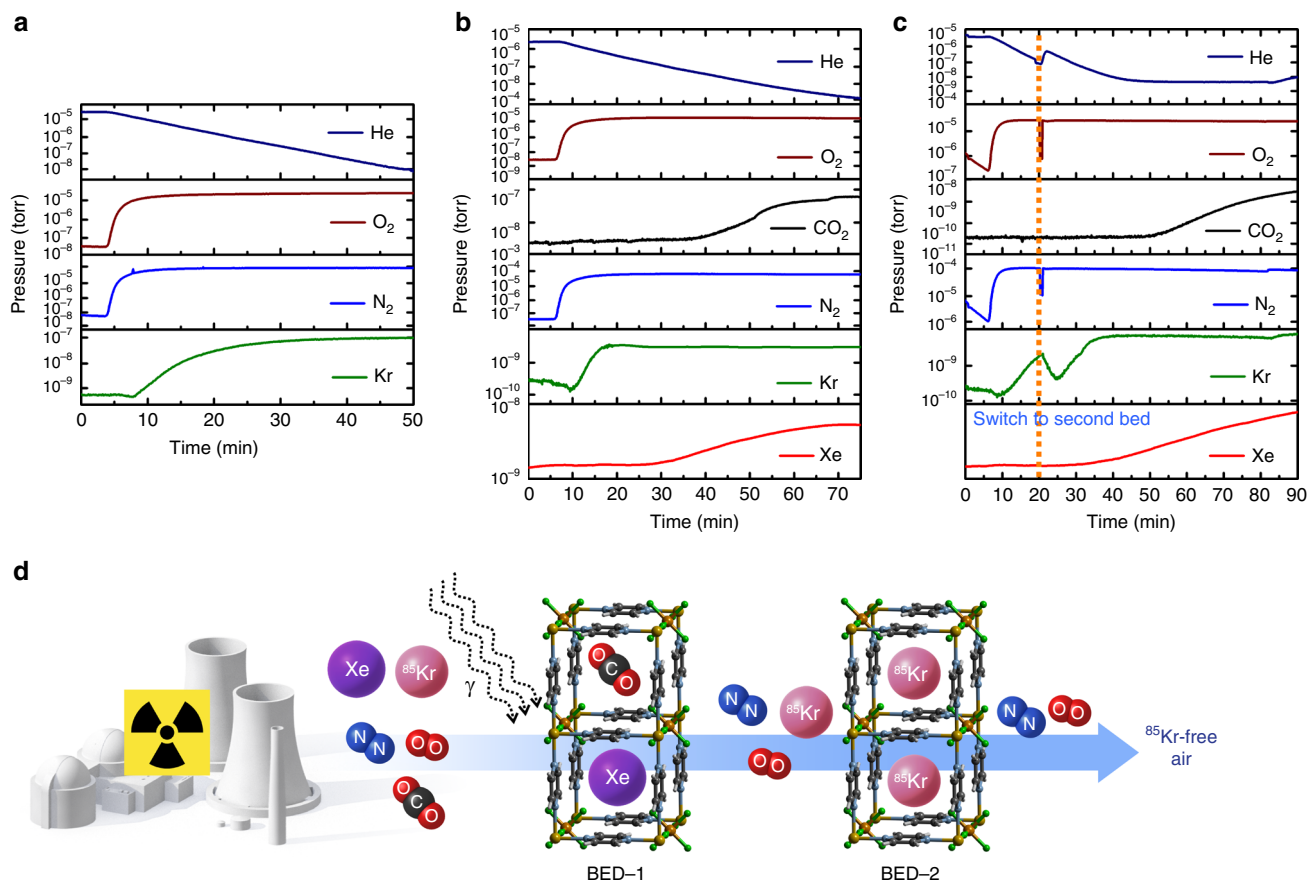


**Fig. 5 Breakthrough curves for SIFSIX-3-Cu.** **a** Single-bed breakthrough experiment using 1000 ppm Kr balanced with dry air. **b** Single-bed breakthrough experiment using 400 ppm Xe and 40 ppm Kr balanced with dry air. **c** Two-bed breakthrough experiment using 400 ppm Xe and 40 ppm Kr balanced with dry air. **d** schematic demonstration of the concept of the two-bed technique for the  $^{85}\text{Kr}$  removal from the UNF.

**Table 1 Xe and Kr separation performance parameters for SIFSIX-3-Cu at 298 K and 1 bar.**

Material	SIFSIX-3-Cu
Xe capacity <sup>a</sup> (mmol/kg)	6.74
Kr capacity <sup>b</sup> (mmol/kg)	0.14
Kr capacity <sup>c</sup> (mmol/kg)	0.15
Kr capacity <sup>d</sup> (mmol/kg)	6.35
Xe/Kr selectivity <sup>e</sup>	4.81
Kr/N <sub>2</sub> selectivity <sup>f</sup>	24.38

Gas mixture 1: 400 ppm Xe, 40 ppm Kr, balanced with dry air

<sup>a</sup>Xe capacity at equilibrium in bed 1 for gas mixture 1.

<sup>b</sup>Kr capacity at equilibrium in bed 2 for gas mixture 1.

<sup>c</sup>Xe/Kr selectivity at equilibrium for bed 1.

Gas mixture 2: 1000 ppm Kr, balanced with dry air

<sup>d</sup>Kr capacity at equilibrium in bed 1 for gas mixture 1.

<sup>e</sup>Kr capacity at equilibrium for gas mixture 2.

<sup>f</sup>Kr/N<sub>2</sub> selectivity at equilibrium for gas mixture 2.

demonstrated by using a two-bed breakthrough technique at ambient conditions. SIFSIX-3-Cu successfully captures Xe in the first bed, while high purity Kr gas is captured in the second bed using the same material. We attribute the remarkable performance of SIFSIX-3-M family to the narrow pore size as well as the high polarizability of  $\text{SiF}_6^{2-}$  anions. Indeed, modeling studies revealed that the adsorbate localizes between four neighboring  $\text{SiF}_6^{2-}$  pillars within the small pores in this class of materials.

## Methods

**Synthesis.**  $[\text{M}(\text{pyz})_2\text{SiF}_6]$  (SIFSIX-3-M, M = Zn, Cu, Ni, Co, Fe) was synthesized by dissolving 10 mmol of pyrazine ligand (pyz) and 5 mmol of  $\text{MSiF}_6$  salt in 23 mL of methanol and heating the resulting solution at 75 °C for 3 days in a stainless steel Parr autoclave<sup>8,29</sup>. SIFSIX-3-Zn and SIFSIX-3-Co afford colorless and red crystals, respectively; while SIFSIX-3-Cu, SIFSIX-3-Ni, and SIFSIX-3-Fe afford blue, pale blue, and yellow crystalline powders, respectively. All structures possess six coordinated saturated metal centers that serve as 6-connected nodes with **pcu** topology through four equatorial pyrazine linkers and 2 axial  $\text{SiF}_6^{2-}$  anion pillars to form the 3D-pillared square-grid nets.

**Gamma irradiation measurements.** The MIT gamma irradiation facility, managed by the MIT Radiation Protection Program (RPP), houses a Gammacell 220 Excel self-shielded high dose-rate gamma ray irradiator (Supplementary Fig. 1) manufactured by MDS Nordion. The unit was manufactured in Canada by MDS Nordion on 13/10/2003 and contained an initial quantity of Cobalt-60 of 23,654 Curies (375.2 TBq) (Supplementary Fig. 2). The Co-60 sources are contained within a lead biological shield which allows for the safe use of the irradiator by trained radiation workers.

The Co-60 sources are arranged in a circle allowing for a uniform dose to the materials being irradiated. The samples are loaded in the sample irradiation chamber and lowered by elevator to the Co-60 source array. The inside dimensions of the chamber are 6.10 in (15.49 cm) diameter and 8.06 in (20.47 cm) high. The current chamber dose rate is 4235 Rads/min (42.35 Gy/min). The original chamber dose rate was 32,228 Rads/min (322.28 Gy/min).

**Beta irradiation measurements.** Experiments were performed at MIT's High Voltage Research Laboratory (HVRL), which houses a continuous-wave Van de Graaff electron accelerator capable of producing electron kinetic energies of 1.5–3.0 MeV at beam currents of up to 30  $\mu\text{A}$ . Samples were irradiated with 1.5 MeV electrons beam at a dose rate of 50 kGy/h.

**Powder X-ray diffraction measurements after gamma irradiation.** The powder X-ray diffraction (PXRD) was collected on the PANalytical X'Pert Pro using 1.8 kW sealed X-ray tube source and Cu target. In order to solve the XRD data we use high score plus program to open the data and we used Rietveld and Pawley fitting methods.

### Data availability

All data needed to evaluate the conclusions of this paper are present in the paper and/or Supplementary Information. The source data underlying Figs. 3a–f, 4a, and 5a–c and Supplementary Figs. 3–7, 9, 10, 12–17, 19–22, and 30, CAR files that were used to make the different binding site pictures in Supplementary Figs. 23–29 and XYZ files containing the atomic coordinates corresponding to the Xe and Kr binding site pictures in Fig. 4b, c are provided as Source Data files. All source data are available from the corresponding author (S.K.E.) by request. Source data are provided with this paper.

Received: 23 October 2019; Accepted: 30 April 2020;

Published online: 18 June 2020

### References

- Banerjee, D. et al. Potential of metal–organic frameworks for separation of xenon and krypton. *Acc. Chem. Res.* **48**, 211–219 (2015).
- Banerjee, D., Simon, C. M., Elsaidi, S. K., Haranczyk, M. & Thallapally, P. K. Xenon gas separation and storage using metal–organic frameworks. *Chem* **4**, 466–494 (2018).
- Riley, B. J., Vienna, J. D., Strachan, D. M., McCloy, J. S. & Jerden, J. L. Materials and processes for the effective capture and immobilization of radioiodine: a review. *J. Nucl. Mater.* **470**, 307–326 (2016).
- Zhang, X. et al. Confinement of iodine molecules into triple-helical chains within robust metal–organic frameworks. *J. Am. Chem. Soc.* **139**, 16289–16296 (2017).
- Soelberg, N. R. et al. Radioactive iodine and krypton control for nuclear fuel reprocessing facilities. *Sci. Technol. Nucl. Ins.* **2013**, 1–12 (2013).
- Banerjee, D. et al. Metal–organic framework with optimally selective xenon adsorption and separation. *Nat. Commun.* **7**, 11831 (2016).
- Mohamed, M. H. et al. Hybrid ultra-microporous materials for selective xenon adsorption and separation. *Angew. Chem. Int. Ed.* **55**, 8285–8289 (2016).
- Elsaidi, S. K. et al. Effect of ring rotation upon gas adsorption in SIFSIX-3-M (M = Fe, Ni) pillared square grid networks. *Chem. Sci.* **8**, 2373–2380 (2017).
- Chen, X. et al. Direct observation of Xe and Kr adsorption in a Xe-selective microporous metal–organic framework. *J. Am. Chem. Soc.* **137**, 7007–7010 (2015).
- Wu, T., Feng, X., Elsaidi, S. K., Thallapally, P. K. & Carreon, M. A. Zeolitic imidazolate framework-8 (ZIF-8) membranes for Kr/Xe separation. *Ind. Eng. Chem. Res.* **56**, 1682–1686 (2017).
- Hulvey, Z. et al. Noble gas adsorption in copper trimesate, HKUST-1: an experimental and computational study. *J. Phys. Chem. C.* **117**, 20116–20126 (2013).
- Perry, J. J. et al. Noble gas adsorption in metal–organic frameworks containing open metal sites. *J. Phys. Chem. C.* **118**, 11685–11698 (2014).
- Liu, J., Strachan, D. M. & Thallapally, P. K. Enhanced noble gas adsorption in Ag@MOF-74Ni. *Chem. Commun.* **50**, 466–468 (2014).
- Fernandez, C. A., Liu, J., Thallapally, P. K. & Strachan, D. M. Switching Kr/Xe selectivity with temperature in a metal–organic framework. *J. Am. Chem. Soc.* **134**, 9046–9049 (2012).
- Wang, H. et al. The first example of commensurate adsorption of atomic gas in a MOF and effective separation of xenon from other noble gases. *Chem. Sci.* **5**, 620–624 (2014).
- Bae, Y.-S. et al. High xenon/krypton selectivity in a metal–organic framework with small pores and strong adsorption sites. *Micropor. Mesopor. Mat.* **169**, 176–179 (2013).
- Kancharlappalli, S., Natarajan, S. & Ghanty, T. K. Confinement-directed adsorption of noble gases (Xe/Kr) in MFM-300(M)-based metal–organic framework materials. *J. Phys. Chem. C.* **123**, 27531–27541 (2019).
- Banerjee, D., Elsaidi, S. K. & Thallapally, P. K. Xe adsorption and separation properties of a series of microporous metal–organic frameworks (MOFs) with V-shaped linkers. *J. Mater. Chem. A* **5**, 16611–16615 (2017).
- Liu, J., Thallapally, P. K. & Strachan, D. Metal–organic frameworks for removal of Xe and Kr from nuclear fuel reprocessing plants. *Langmuir* **28**, 11584–11589 (2012).
- Liu, J. et al. A two-column method for the separation of Kr and Xe from process off-gases. *Ind. Eng. Chem. Res.* **53**, 12893–12899 (2014).
- Forrest, K. A. et al. Investigating CO<sub>2</sub> sorption in SIFSIX-3-M (M = Fe, Co, Ni, Cu, Zn) through computational studies. *Cryst. Growth Des.* **19**, 3732–3743 (2019).
- Lee, S.-J. et al. Adsorptive separation of xenon/krypton mixtures using a zirconium-based metal–organic framework with high hydrothermal and radioactive stabilities. *J. Hazard. Mater.* **320**, 513–520 (2016).
- Cadiau, A. et al. Hydrolytically stable fluorinated metal–organic frameworks for energy-efficient dehydration. *Science* **356**, 731–735 (2017).
- Cui, X. L. et al. Pore chemistry and size control in hybrid porous materials for acetylene capture from ethylene. *Science* **353**, 141–144 (2016).
- Cadiau, A., Adil, K., Bhatt, P. M., Belmabkhout, Y. & Eddaoudi, M. A metal–organic framework-based splitter for separating propylene from propane. *Science* **353**, 137–140 (2016).
- Kanoo, P. et al. Unusual room temperature CO<sub>2</sub> uptake in a fluoro-functionalized MOF: insight from Raman spectroscopy and theoretical studies. *Chem. Commun.* **48**, 8487–8489 (2012).
- Nugent, P. et al. Porous materials with optimal adsorption thermodynamics and kinetics for CO<sub>2</sub> separation. *Nature* **495**, 80–84 (2013).
- Uemura, K., Maeda, A., Maji, T. K., Kanoo, P. & Kita, H. Syntheses, crystal structures and adsorption properties of ultramicroporous coordination polymers constructed from hexafluorosilicate ions and pyrazine. *Eur. J. Inorg. Chem.* **2009**, 2329–2337 (2009).
- Elsaidi, S. K. et al. Hydrophobic pillared square grids for selective removal of CO<sub>2</sub> from simulated flue gas. *Chem. Commun.* **51**, 15530–15533 (2015).
- Shekhah, O. et al. Made-to-order metal–organic frameworks for trace carbon dioxide removal and air capture. *Nat. Commun.* **5**, 4228 (2014).
- Yamamoto, T. & Ootsuka, N. Radiation damage of fluorocarbon by krypton-85 beta-rays, (4). *J. Nucl. Sci. Technol.* **19**, 903–917 (1982).
- Chen, L. et al. Separation of rare gases and chiral molecules by selective binding in porous organic cages. *Nat. Mat.* **13**, 954 (2014).
- Allen, F. The Cambridge Structural Database: a quarter of a million crystal structures and rising. *Acta Cryst. B* **58**, 380–388 (2002).
- Desveaux, B. E. et al. CO<sub>2</sub> behavior in a highly selective ultramicroporous framework: insights from single-crystal X-ray diffraction and solid-state nuclear magnetic resonance spectroscopy. *J. Phys. Chem. C.* **123**, 17798–17807 (2019).
- Winger, K., Feichter, J., Kalinowski, M. B., Sartorius, H. & Schlosser, C. A new compilation of the atmospheric 85krypton inventories from 1945 to 2000 and its evaluation in a global transport model. *J. Environ. Radioact.* **80**, 183–215 (2005).
- Moormann, R., Kemp, R. S. & Li, J. Caution is needed in operating and managing the waste of new pebble-bed nuclear reactors. *Joule* **2**, 1911–1914 (2018).
- Banerjee, D. et al. Metal–organic framework with optimally selective xenon adsorption and separation. *Nat. Commun.* **7**, ncomms11831 (2016).
- Thallapally, P. K., Grate, J. W. & Motkuri, R. K. Facile xenon capture and release at room temperature using a metal–organic framework: a comparison with activated charcoal. *Chem. Commun.* **48**, 347–349 (2012).
- Munakata, K., Yamatsuki, S., Tanaka, K. & Fukumatsu, T. Screening test of adsorbents for recovery of krypton. *J. Nucl. Sci. Technol.* **37**, 84–89 (2000).

### Acknowledgements

Authors would like to thank DOE Office of Nuclear Energy for programmatic funding. In particular we thank Dr. Terry Todd (INL), Dr. John Vienna (PNNL), Dr. Robert Jubin (ORNL), Dr. Kimberly Gray (DOE HQ), and Dr. Patricia Paviet (DOE HQ) for programmatic support. Pacific Northwest National Laboratory is a multiprogramming national laboratory operated for the U.S. Department of Energy by Battelle Memorial Institute under Contract DE-AC05-76RL01830. J.L. acknowledges support from the DOE Office of Nuclear Energy's NEUP Program under Grant No. DE-NE0008827. T.P. and B.S. acknowledge the National Science Foundation (Award No. DMR-1607989), including support from the Major Research Instrumentation Program (Award No. CHE-1531590). Computational resources were made available by a XSEDE Grant (No. TG-DMR090028) and by Research Computing at the University of South Florida. The authors would like to thank Dr. Wenqian Xu (ANL) for the helpful suggestions and Michael Gipple (NETL) for his assistance with the figures graphic.

### Author contributions

S.K.E., M.H.M., J.L., P.T., and D.H. conceived the idea and supervised the project. S.K.E. designed and performed the experiments and collected the data related to materials synthesis and characterization, gas sorption and breakthrough experiments. A.S.H. and M.G. performed the irradiation study and the associated PXRD experiments and their interpretation. T.P., S.S., and B.S. performed the modeling studies and the theoretical calculations. S.K.E., M.H.M., and A.S.H. involved in the analyses and interpretation of data. S.K.E. and M.H.M. wrote the paper with the help of J.L., P.T., T.P., B.S., and D.H.

### Competing interests

The authors declare no competing interests.

**Additional information**

**Supplementary information** is available for this paper at <https://doi.org/10.1038/s41467-020-16647-1>.

**Correspondence** and requests for materials should be addressed to S.K.E., P.K.T. or J.L.

**Peer review information** *Nature Communications* thanks Tapan Ghanty and other, anonymous, reviewers for their contributions to the peer review of this work. Peer review reports are available.

**Reprints and permission information** is available at <http://www.nature.com/reprints>

**Publisher's note** Springer Nature remains neutral with regard to jurisdictional claims in published maps and institutional affiliations.



**Open Access** This article is licensed under a Creative Commons Attribution 4.0 International License, which permits use, sharing, adaptation, distribution and reproduction in any medium or format, as long as you give appropriate credit to the original author(s) and the source, provide a link to the Creative Commons license, and indicate if changes were made. The images or other third party material in this article are included in the article's Creative Commons license, unless indicated otherwise in a credit line to the material. If material is not included in the article's Creative Commons license and your intended use is not permitted by statutory regulation or exceeds the permitted use, you will need to obtain permission directly from the copyright holder. To view a copy of this license, visit <http://creativecommons.org/licenses/by/4.0/>.

© The Author(s) 2020

## **Supplementary Information**

**Radiation-resistant metal-organic framework enables efficient separation of krypton fission gas from spent nuclear fuel**

Elsaidi et al.

## Supplementary Note 1. Gamma Irradiation Study

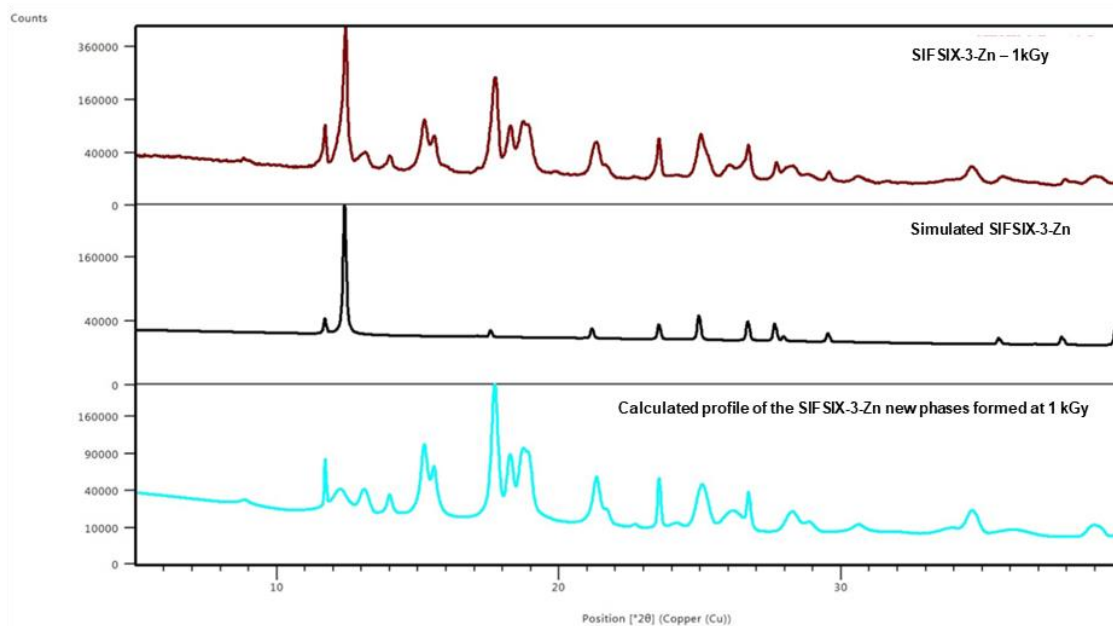


**Supplementary Figure 1.** Gammacell 220 Excel Irradiator.

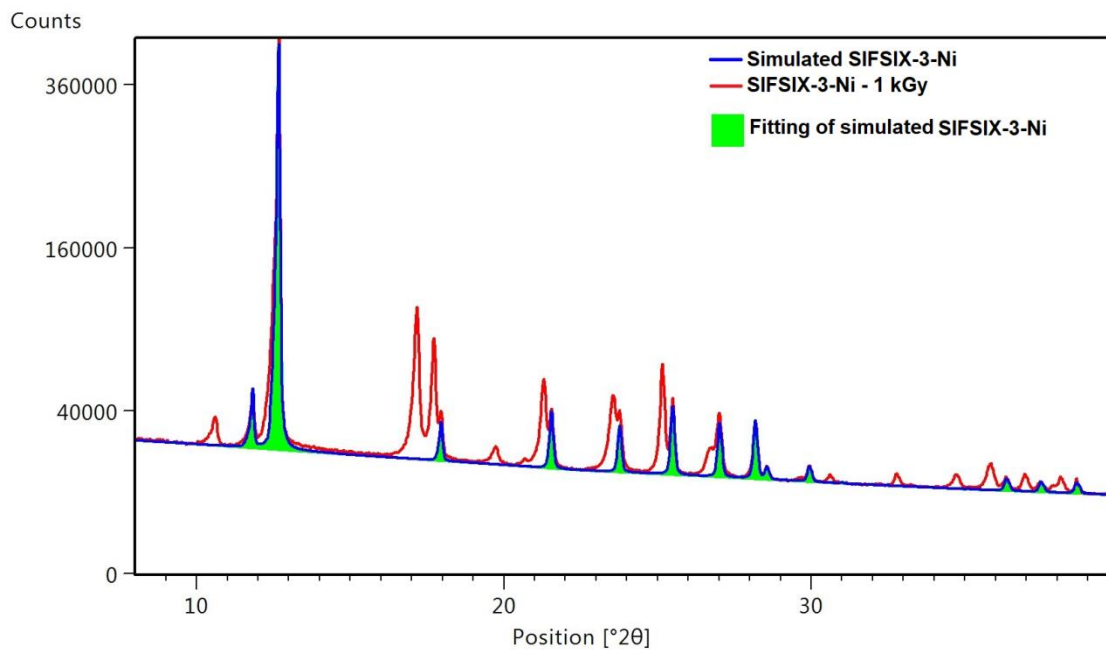


**Supplementary Figure 2.** Original Activity and Weight Specifications.

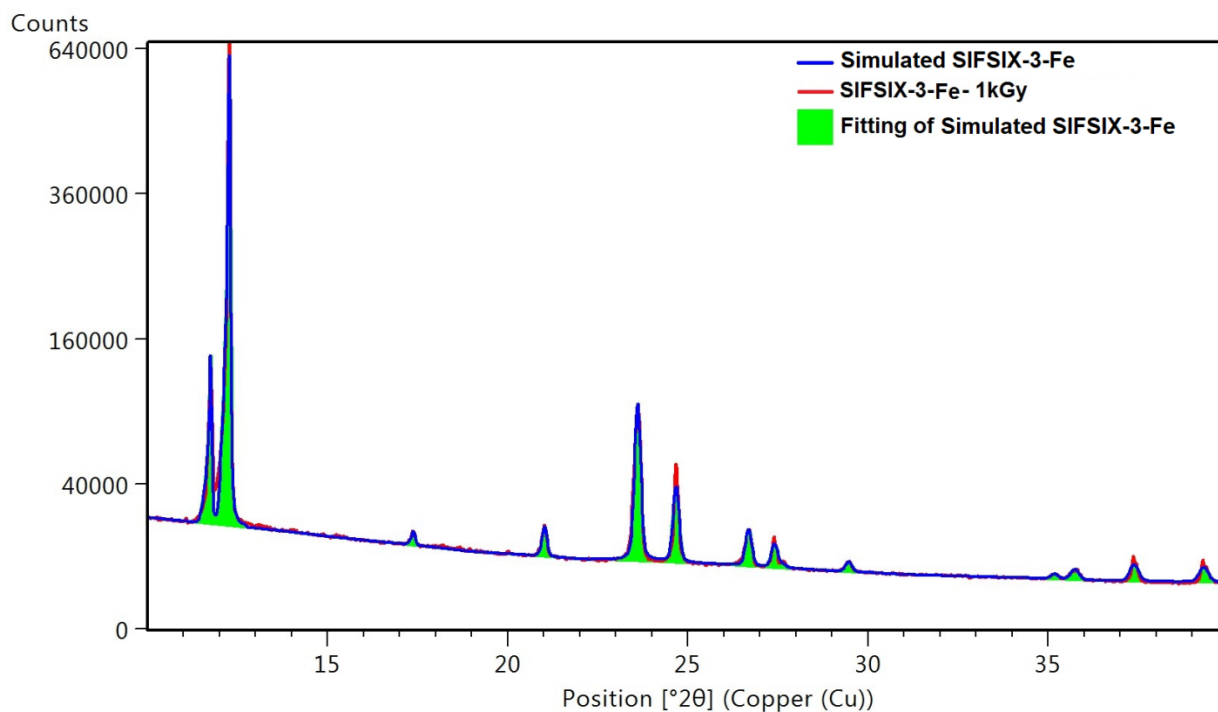
## Supplementary Note 2. Powder X-ray diffraction after gamma irradiation



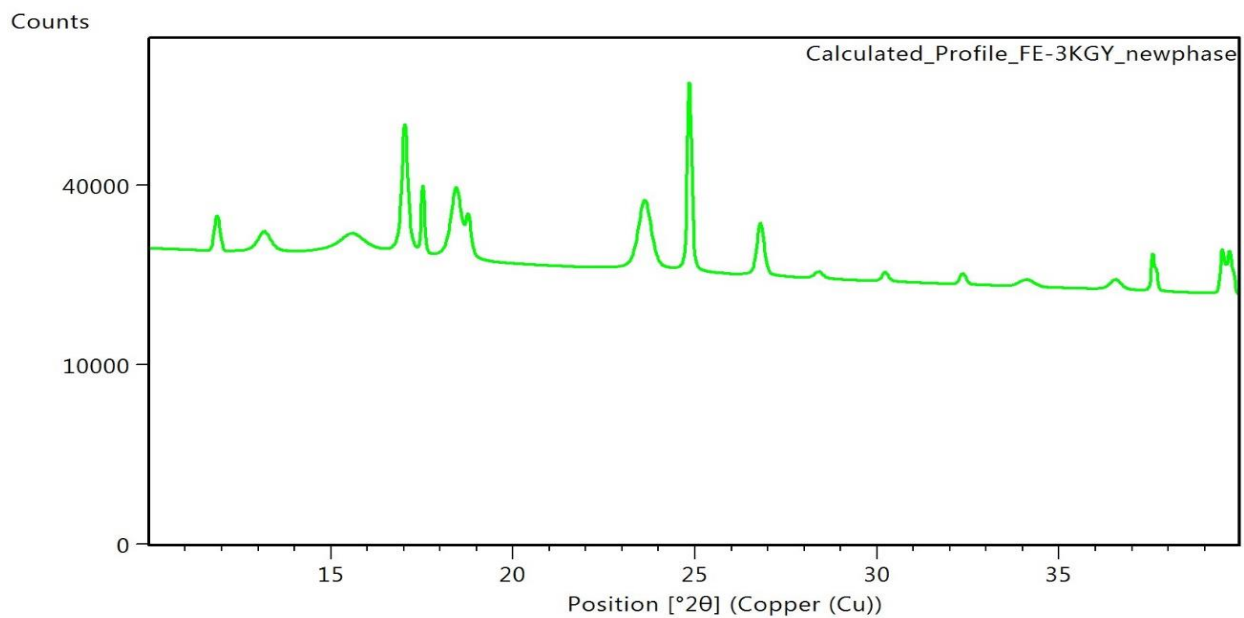
**Supplementary Figure 3.** 2D view comparison between SIFSIX-3-Zn after irradiation with 1 kGy (marron), the crystal structure of SIFSIX-3-Zn (black) and the calculated profile of the new phases (light blue).



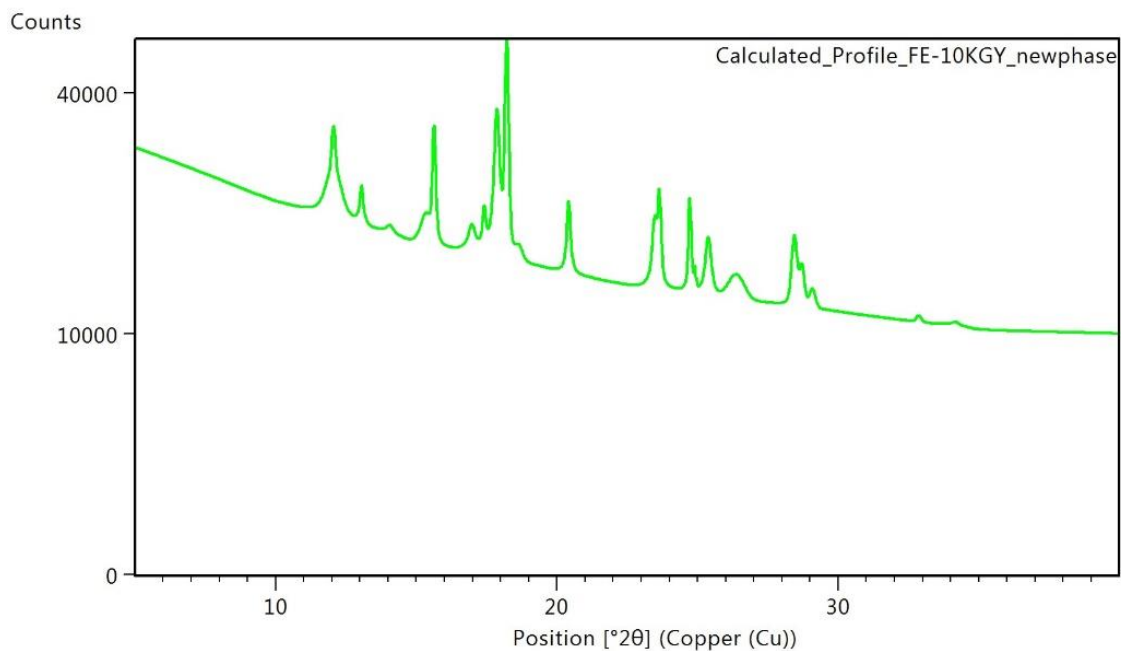
**Supplementary Figure 4.** Pawley fitting method between SIFSIX-3-Ni crystal structure (blue) and irradiated one at 1 kGy (red).



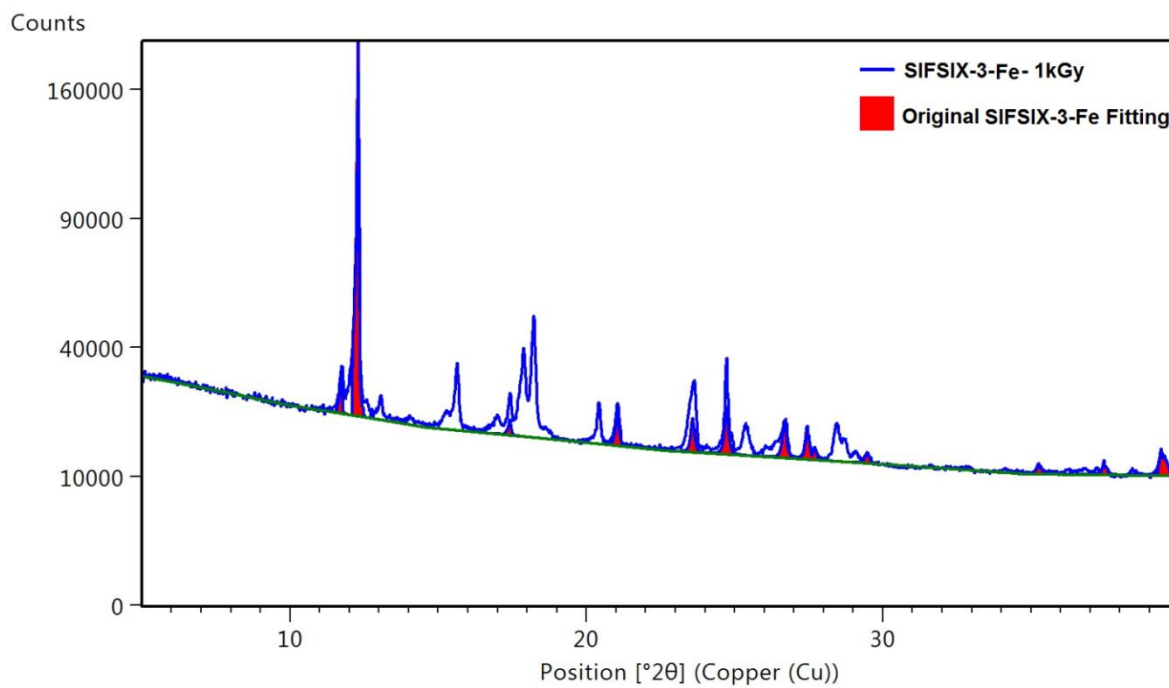
**Supplementary Figure 5.** Rietveld fitting method between SIFSIX-3-Fe crystal structure (blue) and irradiated structure at 1 kGy (red).



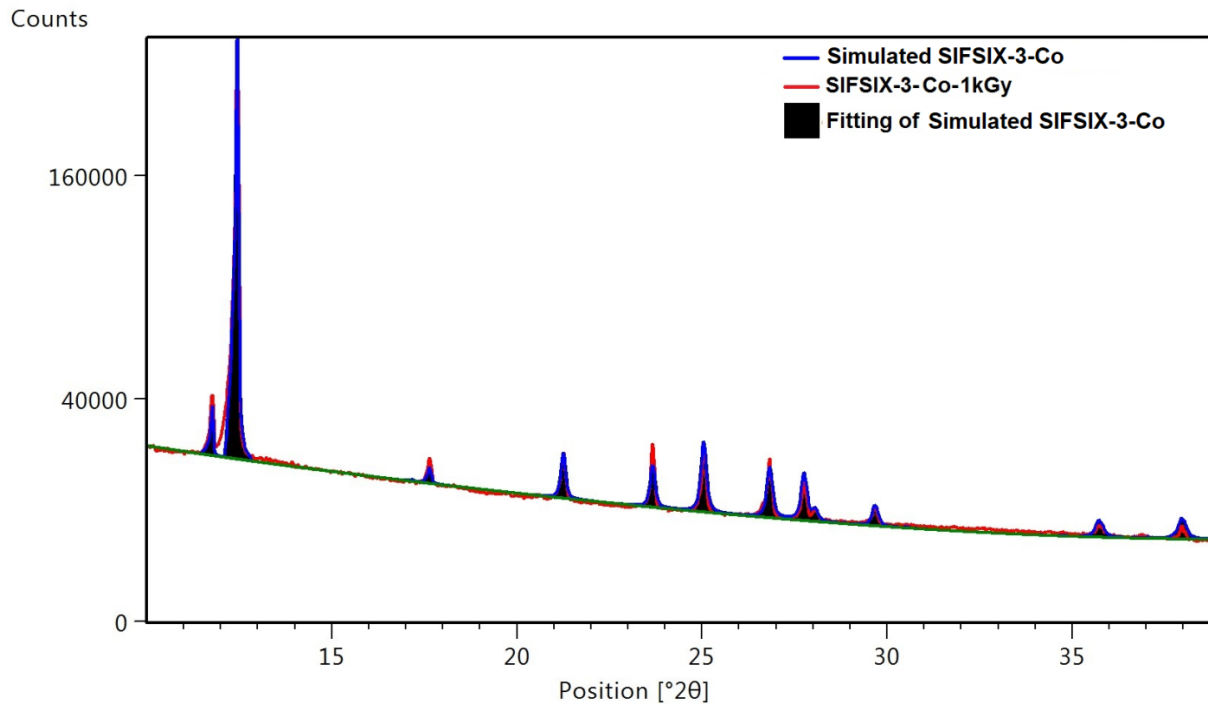
**Supplementary Figure 6.** Calculated profile for the new phase appears after irradiation of SIFSIX-3-Fe with 3 kGy.



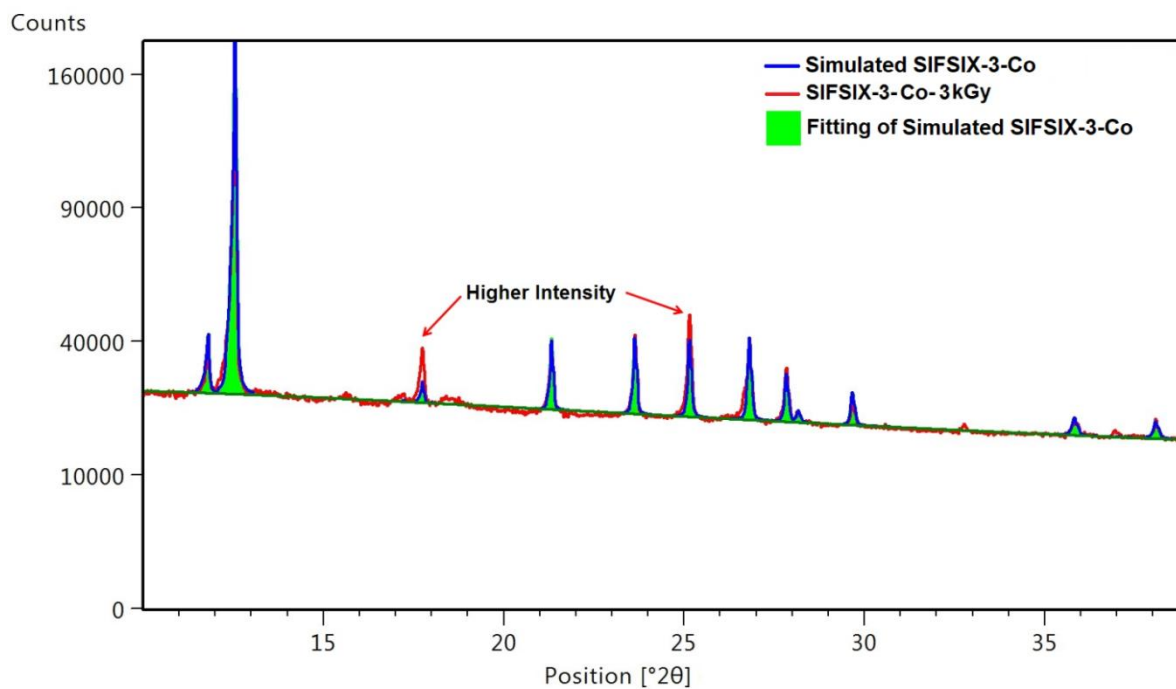
**Supplementary Figure 7.** Calculated profile for the new phase appears after irradiation of SIFSIX-3-Fe with 10 kGy.



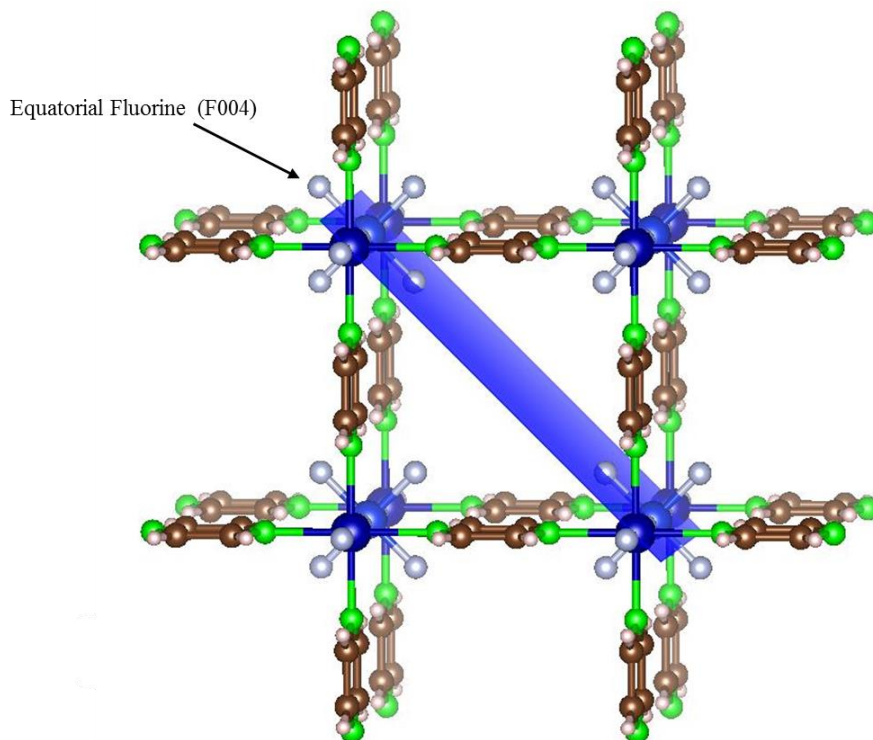
**Supplementary Figure 8.** Pawley fitting method between SIFSIX-3-Fe crystal structure and irradiated one at 10 kGy (green color for the baseline).



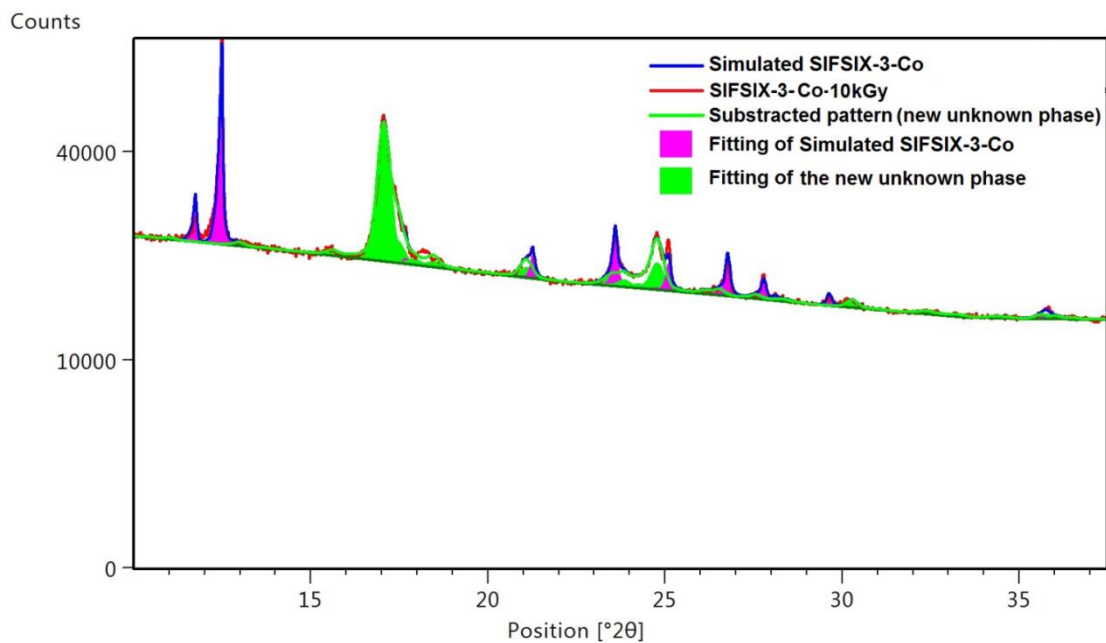
**Supplementary Figure 9.** Rietveld fitting method between SIFSIX-3-Co crystal structure (blue) and irradiated structure at 1 kGy (red). Baseline is shown in green.



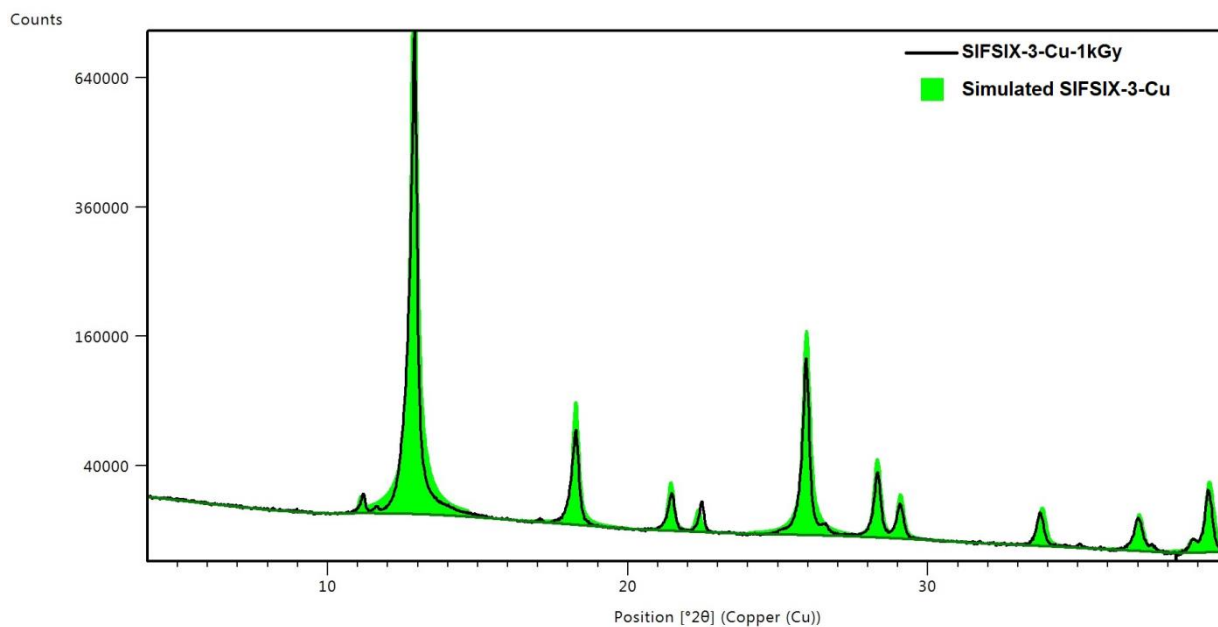
**Supplementary Figure 10.** Rietveld fitting method between SIFSIX-3-Co crystal structure (blue) and irradiated structure at 3 kGy (red).



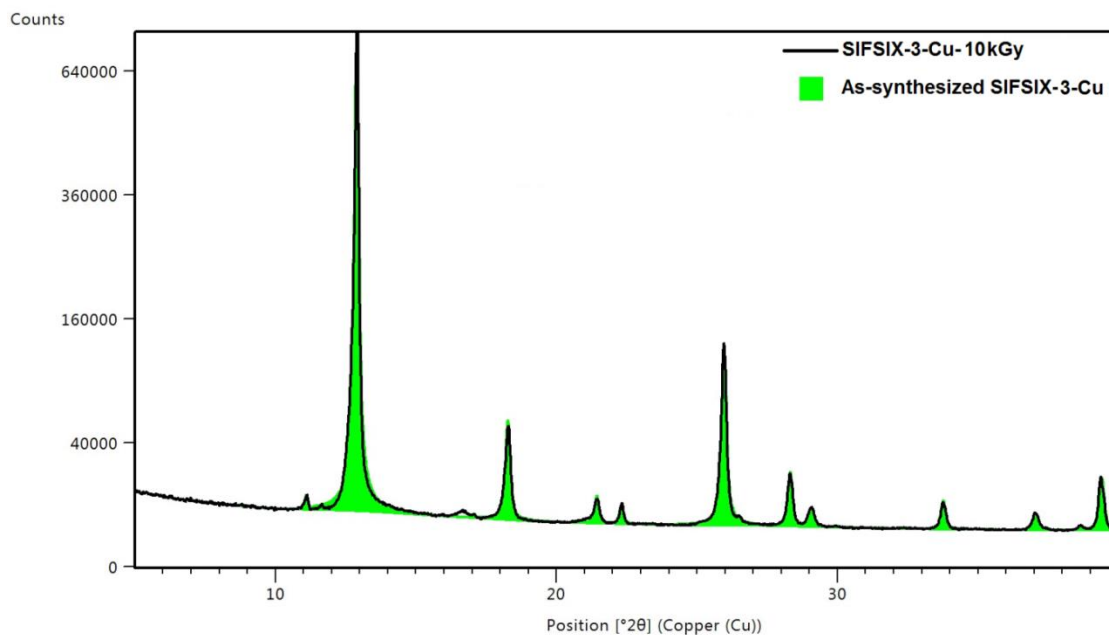
**Supplementary Figure 11.** Crystal structure of SIFSIX-3-Co -110 plane.



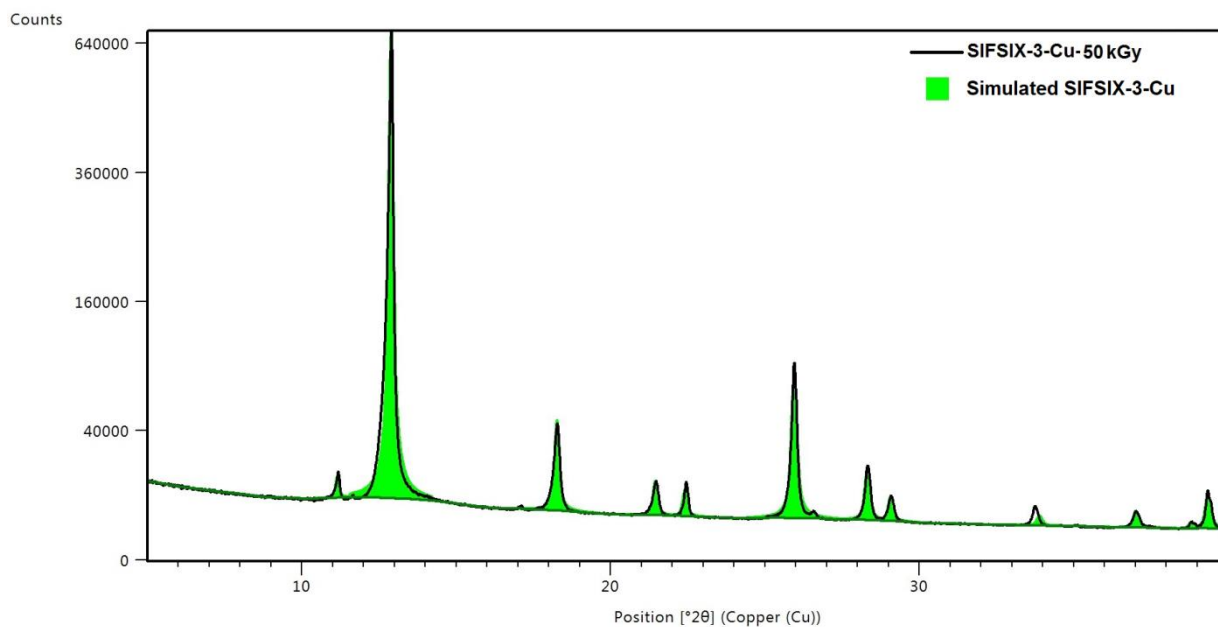
**Supplementary Figure 12.** Pawley fitting method between SIFSIX-3-Co crystal structure (blue) and irradiated structure at 10 kGy (red). To quantitatively analyze the two superimposed XRD patterns we apply both Rietveld and Pawley fitting methods to the SIFSIX-3-Co and the unknown phase, respectively. The Pawley method is used to obtain structure factors by fitting the peak intensities independently.



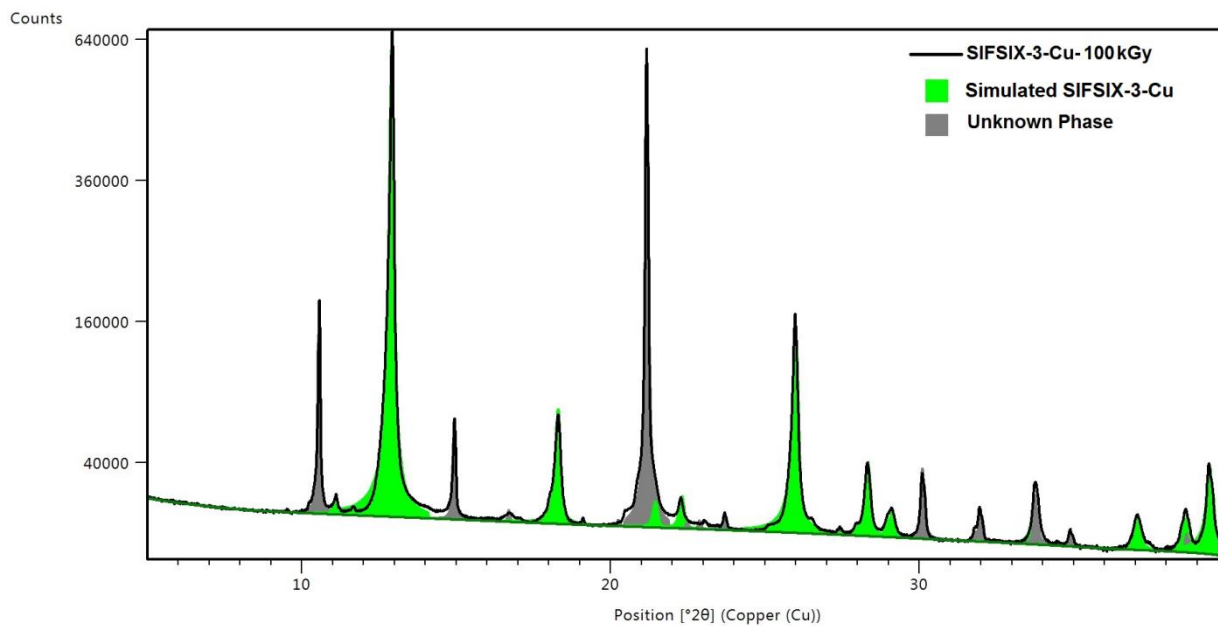
**Supplementary Figure 13.** Pawley fitting method between SIFSIX-3-Cu crystal structure and irradiated one at 1 kGy.



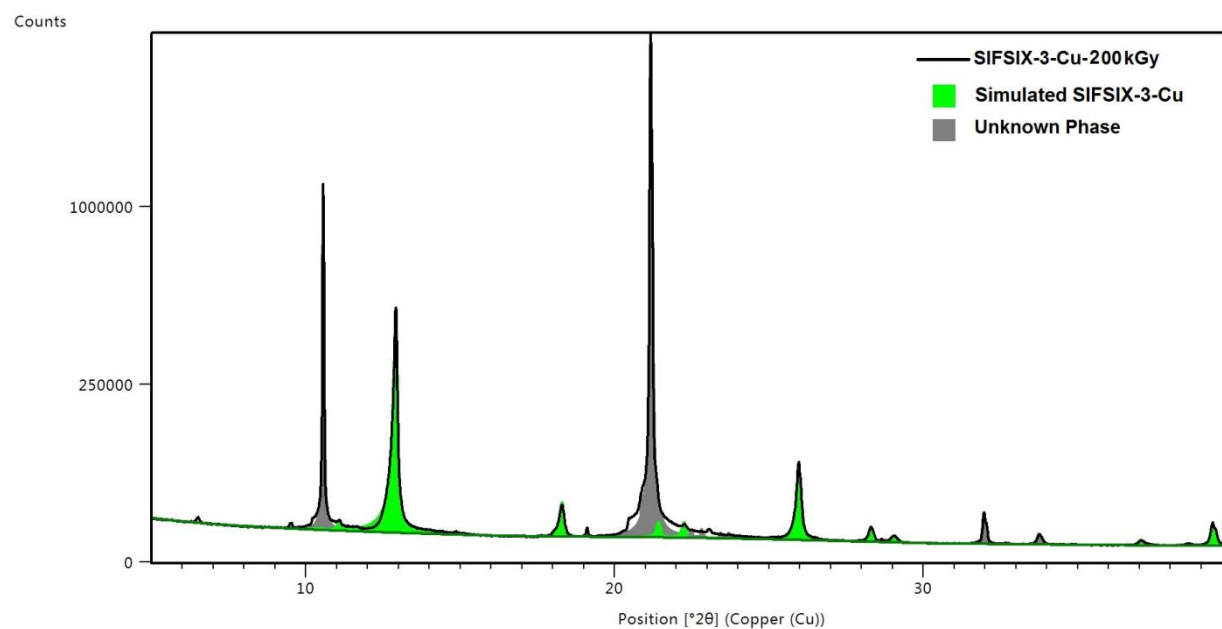
**Supplementary Figure 14.** Pawley fitting method between SIFSIX-3-Cu crystal structure and irradiated one at 10 kGy.



**Supplementary Figure 15.** Pawley fitting method between SIFSIX-3-Cu crystal structure and irradiated one at 50 kGy.



**Supplementary Figure 16.** Pawley fitting method between SIFSIX-3-Cu crystal structure and irradiated one at 100 kGy.



**Supplementary Figure 17.** Pawley fitting method between SIFSIX-3-Cu crystal structure and irradiated one at 200 kGy.

### Supplementary Note 3. Beta Irradiation Study

Beta Dose Calculations from Spent Nuclear Fuel to the SIFSIX-3-Cu MOF:

<sup>85</sup>Kr concentration is reported to be 130 to 1800 TBq/Mg (3.51E3 to 4.86E4 Ci/Mg) of spent fuel.<sup>1</sup> Calculations of absorbed dose from <sup>85</sup>Kr processed in an adsorption matrix is necessary to compare to the damage threshold to that matrix.

<sup>85</sup>Kr's maximum beta energy for the predominate emission (99.57%) is 687 keV and has a corresponding average beta energy of 251 keV. The energy spatial equilibrium dose rate is represented by the total amount of energy deposited per gram of matrix (SIFSIX-3-Cu).<sup>2</sup>

$$\dot{D} = \frac{A}{m} * 3.7E10 * Y * \bar{T}_{\beta} * 3600 \frac{s}{h} * 1.602 * 10^{-10} \frac{Gy}{Mev/g}$$

Where: A is the Activity in Ci,

m is the mass of the matrix volume (assume 1 gm of MOF),

Y is the yield for the transition of interest (assume 1 for beta particles),

$\bar{T}_{\beta}$  is the average kinetic energy of the beta particle (0.251 MeV), and

All others are conversion factors:

3.7E10 dps per curie,

3600 sec per hour, and

$$1.602 * 10^{-10} \frac{Gy}{Mev/g}$$

Simplifying the equation, the dose rate range in Gy/hr in one gram of SIFSIX-3-Cu is as follows:

$$\dot{D} = 5.34E3 * \frac{A Gy}{m h}$$

Thus, the dose rate range for the Kr-85 activity is:

$$\dot{D}(130 TBq) = 1.87E4 \frac{KGy}{hr}$$

$$\dot{D}(1800 TBq) = 2.64E5 \frac{KGy}{hr}$$

Therefore, the radiation dose rate to 1 gm SIFSIX-3-Cu from 1 gm of spent nuclear fuel:

$$\dot{D} = 1.87E-2 \text{ kGy/h (130 TBq/Mg) or}$$

$$\dot{D} = 2.648E-1 \text{ kGy/h (1800 TBq/Mg)}$$

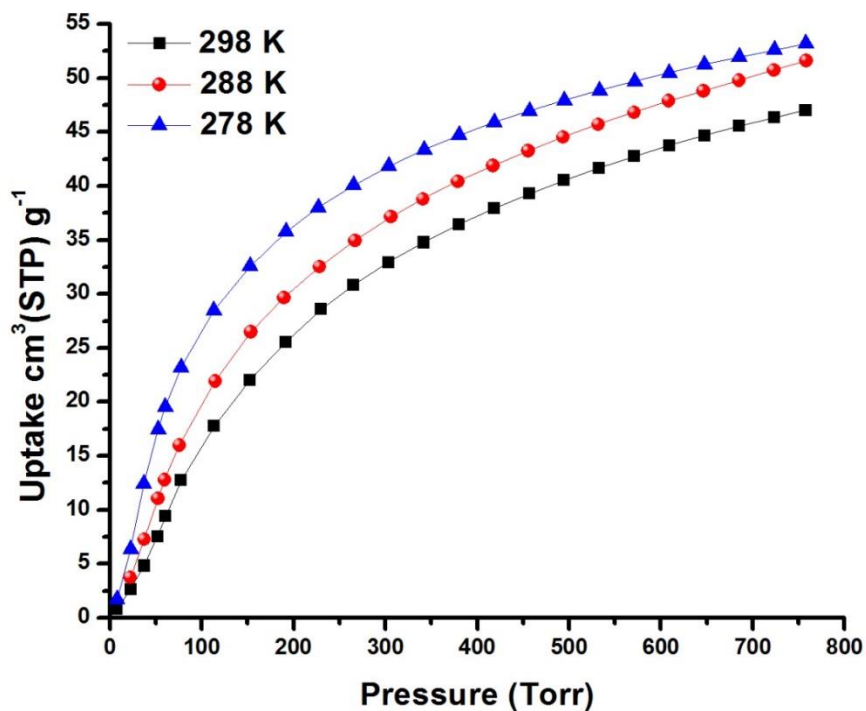
According to the obtained results from both beta and gamma irradiation experiments, SIFSIX-3-Cu is radiation resistant up to 50 KGy. Hence, 1 gm of SIFSIX-3-Cu can separate  $^{85}\text{Kr}$  effectively from 2673.79 g spent nuclear fuel (130 TBq/Mg case) or 188 g spent nuclear fuel (1800 TBq/Mg case) without any crystal structure damage, if keeping all the  $^{85}\text{Kr}$  inside for 1 hour.



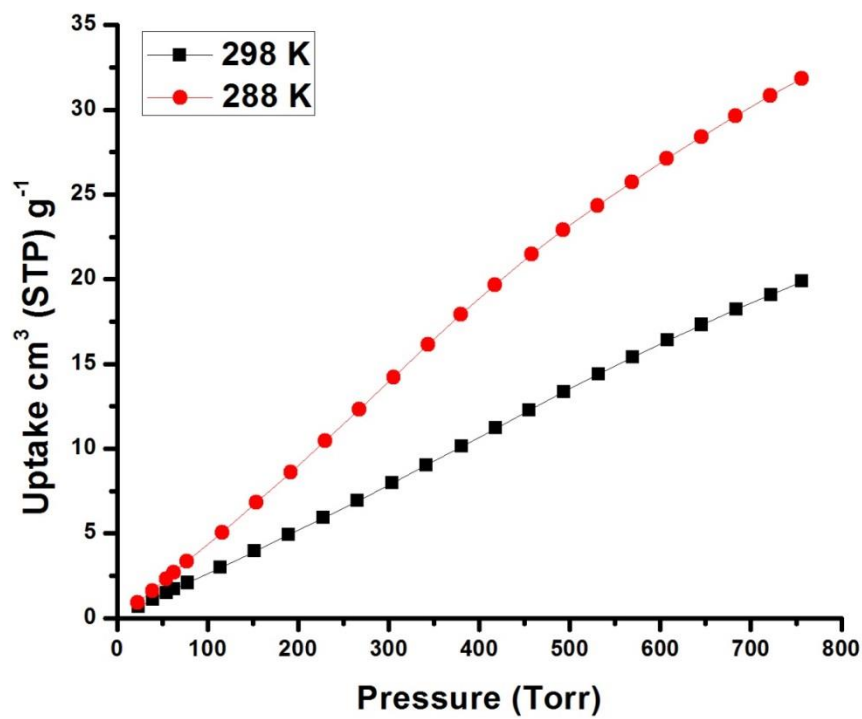
**Supplementary Figure 18.** Van deGraaff electron accelerator.

## Supplementary Note 4. Gas adsorption studies

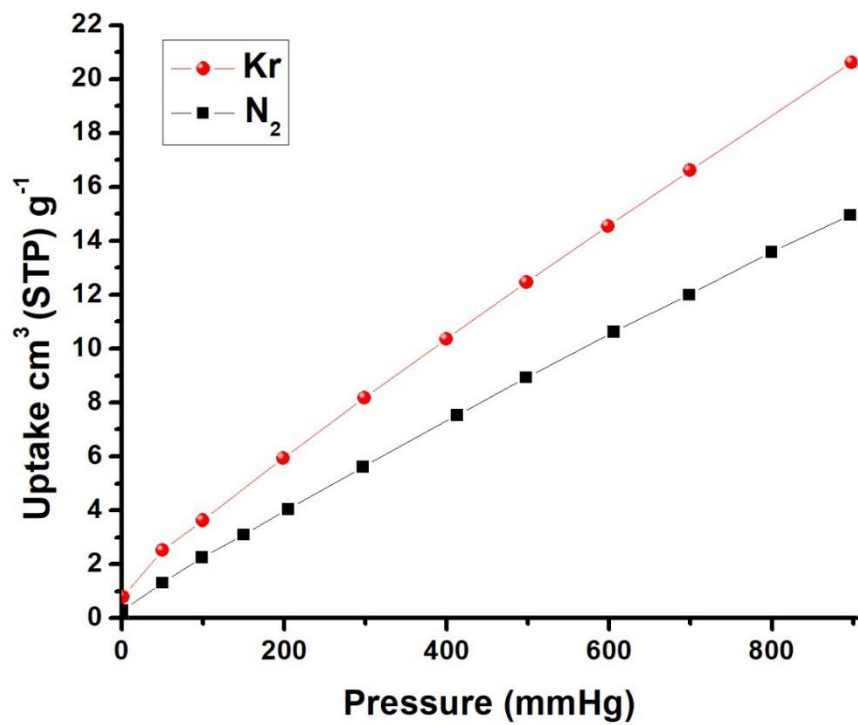
The single-component gas adsorption isotherms were collected on Quantachrome Q1 surface area and gas analyzer instrument within the  $P/P_0$  range of 0–1.0.



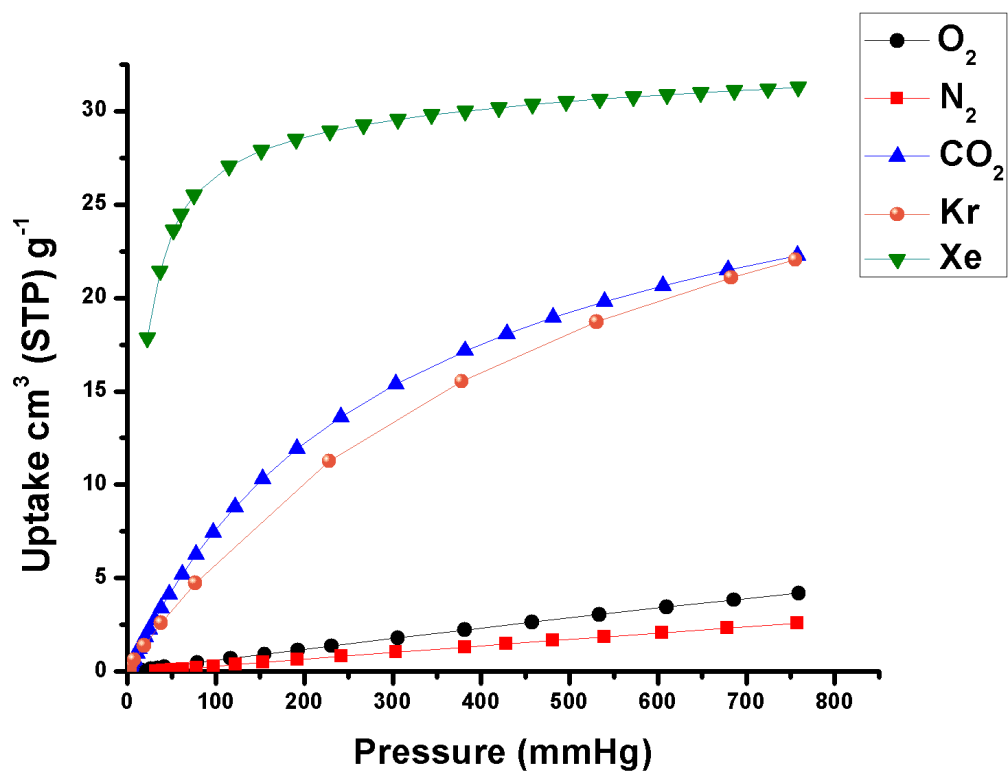
**Supplementary Figure 19.** Single component Xe sorption isotherms for SIFSIX-3-Cu measured at different temperatures.



**Supplementary Figure 20.** Single component Kr sorption isotherms for SIFSIX-3-Cu measured at 298 K and 288 K.



**Supplementary Figure 21.** Single component Kr and N<sub>2</sub> sorption isotherms for Ni-MOF-74 measured at 298 K demonstrating the low Kr/N<sub>2</sub> selectivity.



**Supplementary Figure 22.** Single component Xe, CO<sub>2</sub>, Kr, O<sub>2</sub> and N<sub>2</sub> sorption isotherms for SBMOF-1 measured at 298 K demonstrating extremely low Kr/CO<sub>2</sub> selectivity.

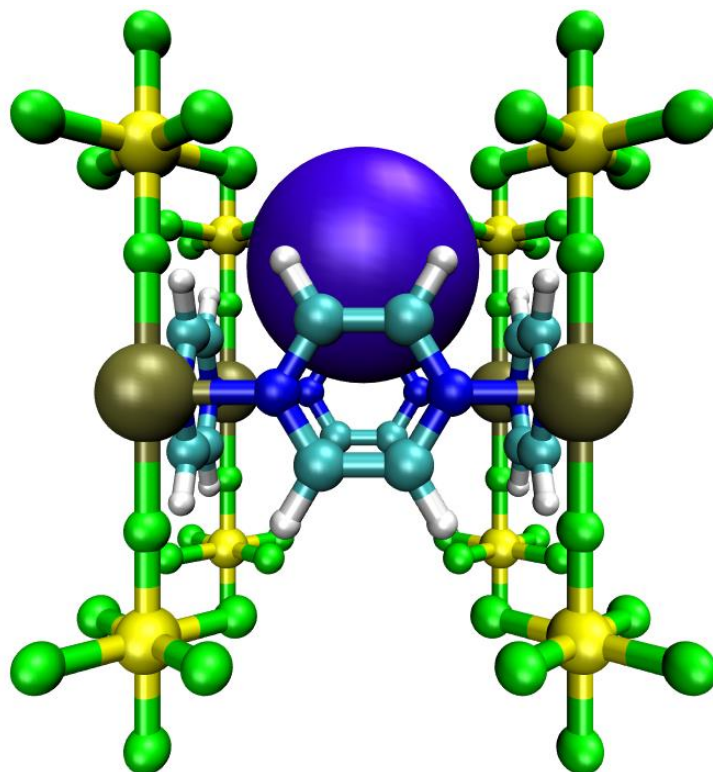
## **Supplementary Note 5. Modeling Studies in SIFSIX-3-Cu**

Since SIFSIX-3-Cu was found to be the most stable analogue when subjected to gamma radiation, it was the focus of molecular simulation studies of Xe and Kr adsorption. To the best of our knowledge, theoretical studies of Xe and Kr adsorption in the Cu variant of SIFSIX-3-M have not been performed earlier.

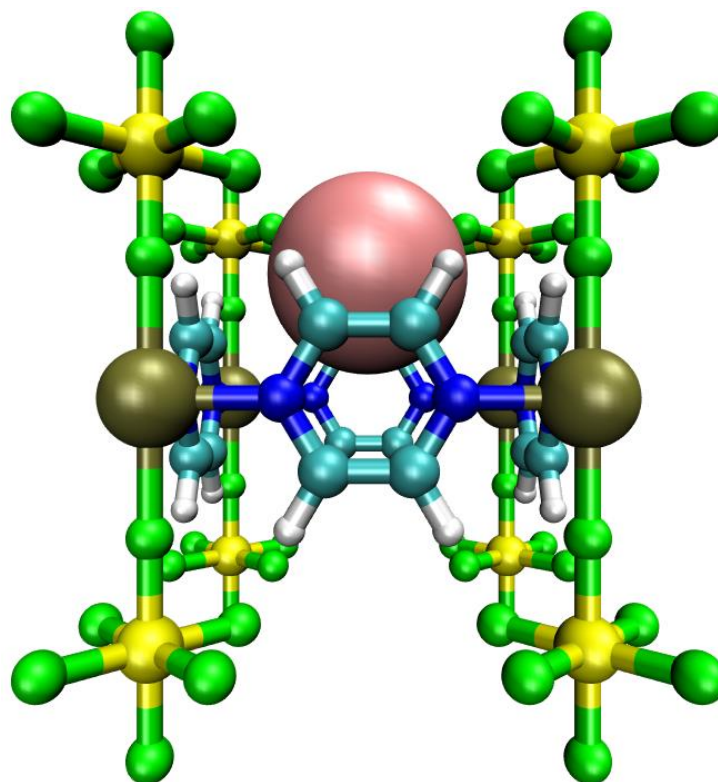
First, the originally published crystal structure of SIFSIX-3-Cu (as taken from reference 3) was fully optimized (i.e., atoms and lattice parameters relaxed) using the Vienna *ab initio* Simulation Package (VASP)<sup>4</sup> (version 5.4.4) with the projector augmented wave (PAW) method<sup>5</sup>, Perdew–Burke–Ernzerhof (PBE) functional,<sup>6</sup> and the DFT-D2 correction method of Grimme.<sup>7</sup> This optimized structure was then used to carry out classical simulated annealing calculations<sup>8</sup> of Xe and Kr in the material to determine the most favorable binding site for the respective adsorbates. These simulations were performed within the  $3 \times 3 \times 3$  supercell of the material through a Monte Carlo process. We note that the crystal structure of SIFSIX-3-Cu was also optimized using the DFT-D3 method of Grimme *et al.*<sup>9</sup> However, the resulting relaxed structure had an energy that was surprisingly higher than that obtained using the DFT-D2 method (–705.5814605 vs –706.2898731 eV). Since the DFT-D2 method generated a crystal structure that was more stable, this optimized structure was therefore utilized for the classical simulations.

The classical force field for SIFSIX-3-Cu, which includes Lennard-Jones 12–6 parameters, point partial charges, and scalar point polarizabilities, was established in previous work<sup>10</sup> and used for the simulations executed herein. Simulated annealing calculations within the canonical (*NVT*) ensemble were implemented for a single Xe and Kr atom, respectively, in SIFSIX-3-Cu using polarizable potentials that were developed previously for the individual adsorbates.<sup>11</sup> These simulations started at an initial temperature of 500 K, and this temperature was scaled by a factor of 0.99999 after every 1,000 Monte Carlo steps. The simulations continued until the temperature of the MOF–adsorbate system decreased below 10 K. These calculations were performed using the Massively Parallel Monte Carlo (MPMC) code.<sup>12</sup>

The global minimum for both Xe and Kr in SIFSIX-3-Cu was identified as localization between the equatorial fluorine atoms of four neighboring  $\text{SiF}_6^{2-}$  anions within the square corridor (Supplementary Figs 23 and 24). The greater atomic radius for Xe relative to Kr (1.08 vs 0.88 Å) afforded a better fit within the pores and generally shorter distances between the adsorbate and the equatorial F atoms ( $r = 0.42$  Å), which results in stronger interactions with the host. After subtracting the distance corresponding to the atomic radii of the adsorbate and F atoms from the distance measured between the two center-of-masses, the Xe···F distances for the annealed position were measured to be 1.94, 1.96, 1.98, and 2.00 Å, while distances of 2.14, 2.18, 2.22, and 2.25 Å were measured for the Kr···F interaction.



**Supplementary Figure 23.** Molecular illustration of the most favorable binding site for Xe in **SIFSIX-3-Cu** (side view) as determined from simulated annealing calculations. Atom colors: C = cyan, H = white, N = blue, F, = green, Si = yellow, Cu = gold, Xe = violet.



**Supplementary Figure 24.** Molecular illustration of the most favorable binding site for Kr in SIFSIX-3-Cu (side view) as determined from simulated annealing calculations. Atom colors: C = cyan, H = white, N = blue, F = green, Si = yellow, Cu = gold, Kr = pink.

Periodic DFT calculations were also performed to evaluate the adsorption energy ( $\Delta E$ ) for Xe, Kr, CO<sub>2</sub>, N<sub>2</sub>, and O<sub>2</sub> within SIFSIX-3-Cu. These calculations were performed using VASP with the same methods that were employed for optimizing an empty unit cell of the material. The position of a single atom/molecule of each adsorbate was initially optimized within the rigid unit cell of the MOF. Afterward, another optimization was carried out in which the position of all atoms and lattice parameters of the system could fluctuate. The optimized position of a Xe, Kr, CO<sub>2</sub>, N<sub>2</sub>, and O<sub>2</sub> atom/molecule about four neighboring SiF<sub>6</sub><sup>2-</sup> anions within SIFSIX-3-Cu are displayed in Supplementary Figs 25-29. The DFT-optimized positions for Xe and Kr in this material are visually identical to those obtained through simulated annealing calculations (Supplementary Figs 23-24).

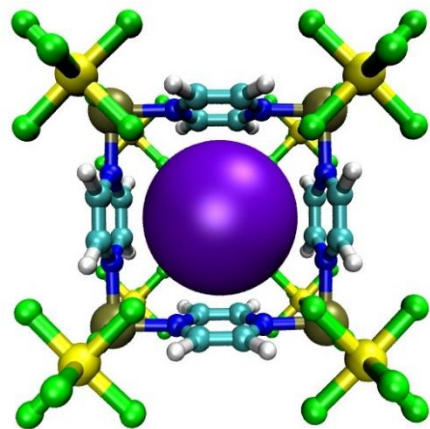
The  $\Delta E$  for the adsorbates localized within the unit cell of SIFSIX-3-Cu were calculated by the following:

$$\Delta E = E(\text{MOF} + \text{Adsorbate}) - E(\text{MOF}) - E(\text{Adsorbate})$$

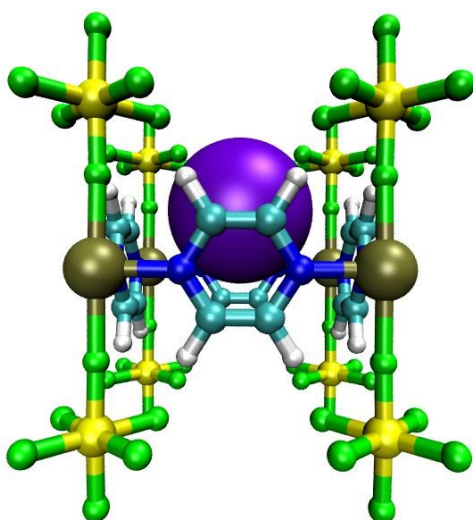
where  $E(\text{MOF} + \text{Adsorbate})$  is the energy of the unit cell of the MOF with the adsorbate,  $E(\text{MOF})$  is the energy of the empty unit cell, and  $E(\text{Adsorbate})$  is the energy of the adsorbate. The calculated  $\Delta E$  values for Xe, Kr, CO<sub>2</sub>, N<sub>2</sub>, and O<sub>2</sub> within SIFSIX-3-Cu are listed in Supplementary Table 1.

**Supplementary Table 1:** Calculated adsorption energies (in kJ mol<sup>-1</sup>) for a single atom/molecule of Xe, Kr, CO<sub>2</sub>, N<sub>2</sub>, and O<sub>2</sub> within the unit cell of SIFSIX-3-Cu as determined from periodic DFT calculations using VASP.

<b>Absorbate</b>	<b><math>\Delta E</math> (kJ mol<sup>-1</sup>)</b>
Xe	-45.93
Kr	-31.14
CO <sub>2</sub>	-58.42
N <sub>2</sub>	-21.01
O <sub>2</sub>	-15.10

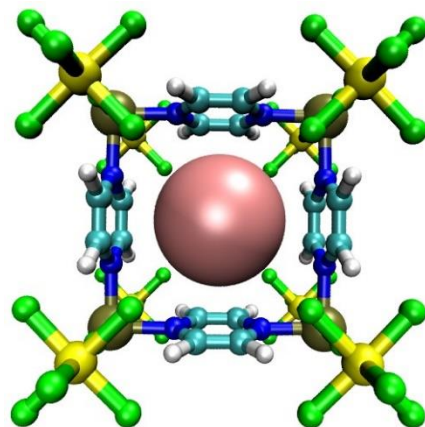


(a)

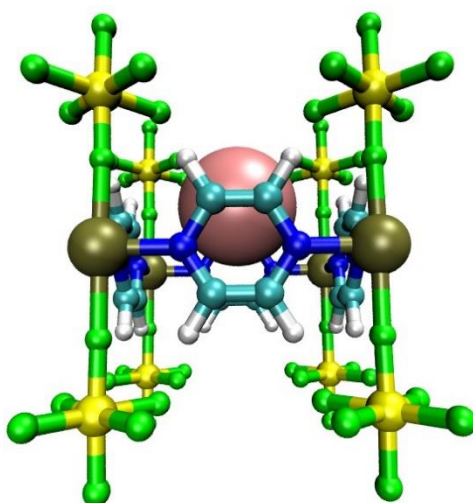


(b)

**Supplementary Figure 25.** Molecular illustration of the most favorable binding site for Xe in SIFSIX-3-Cu as determined from periodic DFT calculations using VASP: (a) top view; (b) side view. Atom colors: C = cyan, H = white, N = blue, F, = green, Si = yellow, Cu = gold, Xe = violet.

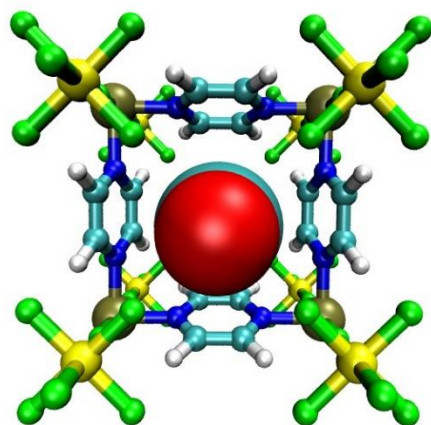


(a)

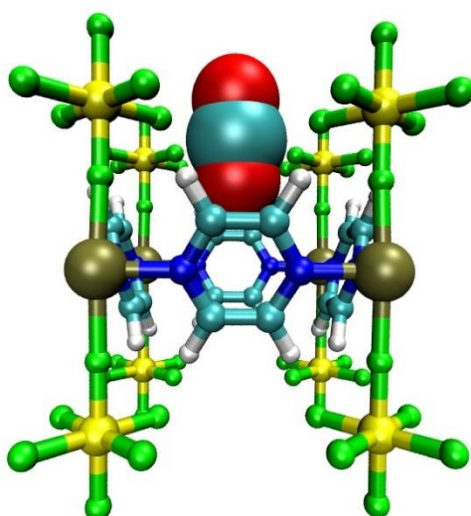


(b)

**Supplementary Figure 26.** Molecular illustration of the most favorable binding site for Kr in SIFSIX-3-Cu as determined from periodic DFT calculations using VASP: (a) top view; (b) side view. Atom colors: C = cyan, H = white, N = blue, F, = green, Si = yellow, Cu = gold, Kr = pink.

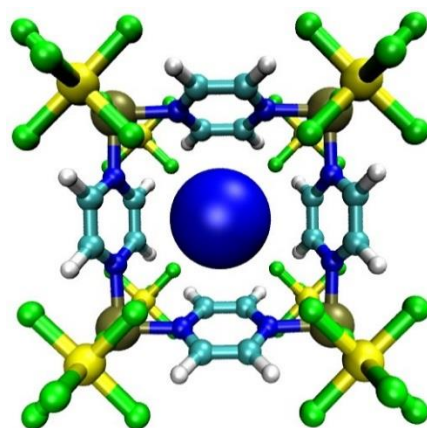


(a)

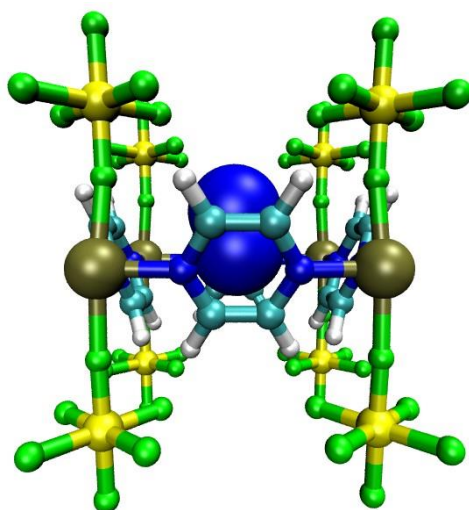


(b)

**Supplementary Figure 27.** Molecular illustration of the most favorable binding site for CO<sub>2</sub> in SIFSIX-3-Cu as determined from periodic DFT calculations using VASP: (a) top view; (b) side view. Atom colors: C = cyan, H = white, N = blue, O = red, F, = green, Si = yellow, Cu = gold.

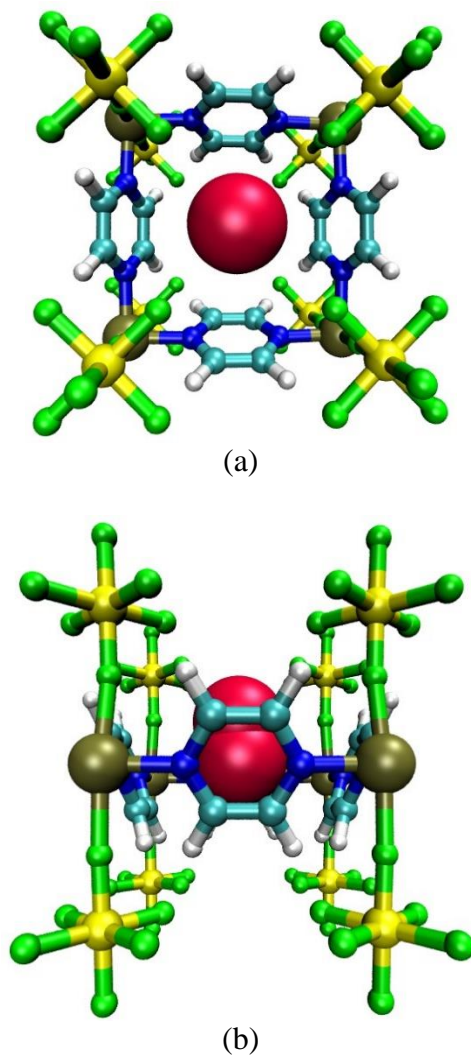


(a)



(b)

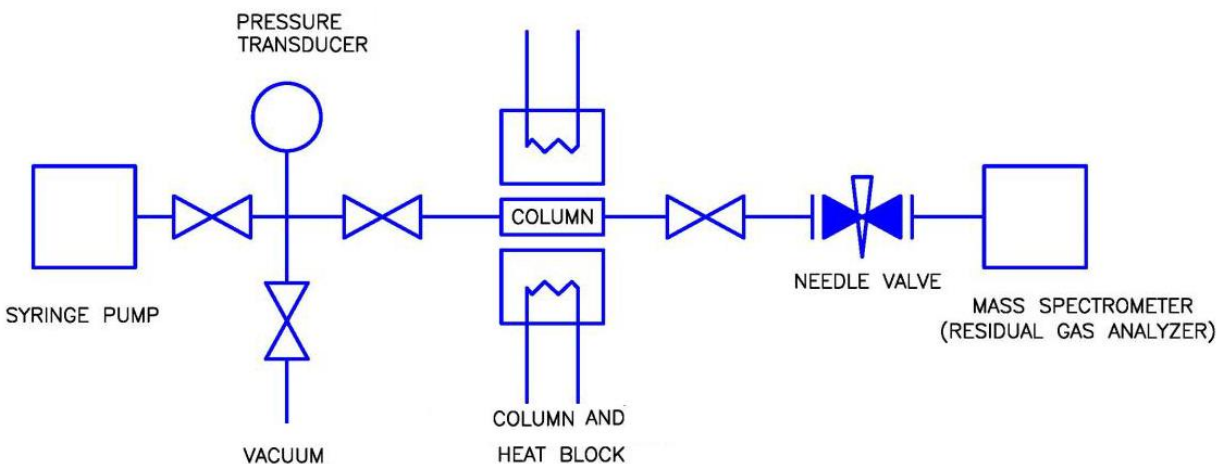
**Supplementary Figure 28.** Molecular illustration of the most favorable binding site for N<sub>2</sub> in SIFSIX-3-Cu as determined from periodic DFT calculations using VASP: (a) top view; (b) side view. Atom colors: C = cyan, H = white, N = blue, F, = green, Si = yellow, Cu = gold.



**Supplementary Figure 29.** Molecular illustration of the most favorable binding site for  $O_2$  in SIFSIX-3-Cu as determined from periodic DFT calculations using VASP: (a) top view; (b) side view. Atom colors: C = cyan, H = white, N = blue, O = red, F = green, Si = yellow, Cu = gold.

## **Supplementary Note 6. Single-bed breakthrough experiments:**

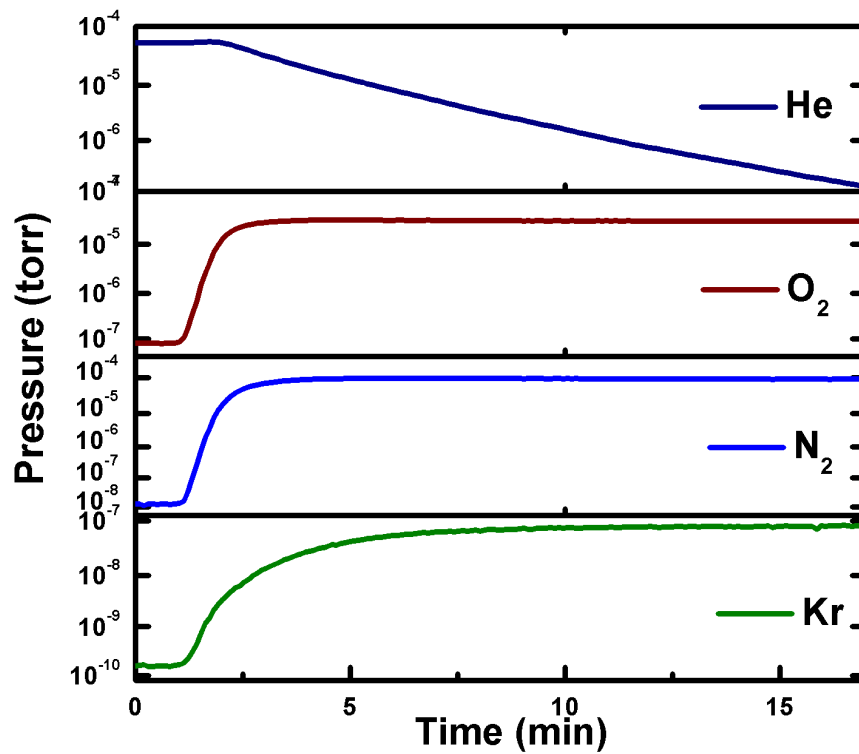
Experimental single-bed breakthrough measurements were conducted by packing about 1 g of adsorbent sample in the column. SIFSIX-3-Cu was activated under vacuum at room temperature for 12 hr and at 55 °C for another 12 hr. Pressurization of the column-containing adsorbent material was accomplished by syringe pump (Teledyne ISCO) directly connected to the system. An inline pressure transducer was used to verify column pressure. The column was cooled to room temperature and the pure He gas was initially flowed to a Stanford Research Residual Gas Analyzer (RGA) for first three minutes, after which the flow of He is stopped and flow of the gas mixture is introduced to the fixed bed column containing the adsorbent sample with flow rate of 5 ml/min and total pressure of 1 bar at room temperature. Effluent gases were thereby tracked with the RGA, while the gases breaking through the column were indicated by an increase in the pressure. This ran for the next 2-4 hours. The experimental set-up of the single-bed breakthrough experiment is presented in Supplementary Scheme 1.



**Supplementary Scheme 1.** Schematic representation of the single column breakthrough experiment set-up combined with the mass spectrophotometer.

## **Supplementary Note 7. Two-bed breakthrough experiments for Xe/Kr gas mixture**

The breakthrough apparatus used in the current experiments was previously described in literature.<sup>13</sup> It consists of two adsorption beds in series equipped with two separate temperature controllers and one common mass spectrometer. Mass flow controllers are used to control the gas flow through the columns by adjusting the valve in order to switch the system between one-bed or two-bed regimes. Both columns have the same diameter of 10 mm and length of 100 mm and the voidage of the packed bed  $\epsilon$  equals to 0.5. The pressurization of the two beds containing the SIFSIX-3-Cu was implemented by syringe pump (Teledyne ISCO) directly connected to the system. An inline pressure transducer was used to verify column pressure. At the other side, Stanford Research Residual Gas Analyzer (RGA) was connected to the system in order to track the effluent gases, while the gases breaking through the two-columns were indicated by an increase in the pressure. The simulated nuclear gas-mixture is composed of 400 ppm Xe, 40 ppm Kr, balanced with air. The gas-flow can be switched between one-bed mode and two bed mode by adjusting the valve in between the beds. Prior to the breakthrough experiments, adsorbent sample was activated at appropriate temperature under He flow and the total flow rate was kept constant until the start of the breakthrough experiment. The inlet and outlet pressure was monitored by pressure gauge and kept constant at 1 bar. All flow rate for both the gas-mixture and He flow was 5 ml/min. Prior to the two-bed experiment, gas-mixture was flown through bed one only to evaluate the Xe adsorption capacity under dynamic condition and current setup. For the two-bed experiment, once the Kr (and other gaseous components) breaks through the bed and reaches equilibrium concentration, the resultant gas-flow was switched to the 2<sup>nd</sup> bed using the valve in between the bed. Once Kr and other gaseous component breakthrough from the 2<sup>nd</sup> bed as recorded in the mass spectrometer, the valve to the 2<sup>nd</sup> bed was turned off, so that gas-mix breaking through the 1<sup>st</sup> bed only reaches the mass-spectrometer. The feed gas tank (400 ppm Xe, 40 ppm Kr, balance air, also termed as simulated off-gas stream) were purchased from Advanced Specialty Gases (Reno, NV).



**Supplementary Figure 30.** Single-bed breakthrough experiment using 1000 ppm Kr balanced with dry air for Ag mordenite demonstrating the low Kr/N<sub>2</sub> selectivity.

## Supplementary References

1. Wingera, K.; Feichtera, J.; Kalinowskib, M.B.; Sartoriusc, H.; Schlosser, C. *Journal of Environmental Radioactivity*, **2005**, *80*, 183–215.
2. Attix, F., H. **2004** WILEY-VCH Verlag GmbH & Co. KGaA. ISBN:9780471011460.
3. Shekhah, O.; Belmabkhout, Y.; Chen, Z.; Guillerm, V.; Cairns, A.; Adil, K.; Eddaoudi, M. *Nat. Commun.* **2014**, *5*, 4228.
4. (a) Kresse, G.; Hafner, J. *Phys. Rev. B* **1993**, *47*, 558–561. (b) Kresse, G.; Hafner, J. *Phys. Rev. B* **1994**, *49*, 14251–14269. (c) Kresse, G.; Furthmüller, J. *Comput. Mater. Sci.* **1996**, *6*, 15–50. (d) Kresse, G.; Furthmüller, J. *Phys. Rev. B.* **1996**, *54*, 11169–11186.
5. (a) Blöchl, P. E. *Phys. Rev. B* **1994**, *50*, 17953. (b) Kresse, G.; Joubert, D. *Phys. Rev. B* **1999**, *59*, 1758.
6. (a) Perdew, J. P.; Burke, K.; Ernzerhof, M. *Phys. Rev. Lett.* **1996**, *77*, 3865. (b) Perdew, J. P.; Burke, K.; Ernzerhof, M. *Phys. Rev. Lett.* **1997**, *77*, 1396.
7. Grimme, S. *J. Comput. Chem.* **2006**, *27*, 1787–1799.
8. Grimme, S.; Antony, S.; Ehrlich, S.; Krieg, H. *J. Comput. Chem.* **2010**, *132*, 154104.
9. Kirkpatrick, S.; Gelatt, C. D.; Vecchi, M. P. *Science* **1983**, *220*, 671–680.
10. Forrest, K. A.; Pham, T.; Space, B. *CrystEngComm* **2017**, *19*, 3338–3347.
11. Mohamed, M. H.; Elsaidi, S. K.; Pham, T.; Forrest, K. A.; Schaef, H. T.; Hogan, A.; Wojtas, L.; Xu, W.; Space, B.; Zaworotko, M. J.; Thallapally, P. K. *Angew. Chem. Int. Ed.* **2016**, *55*, 8285–8289.
12. Belof, J. L.; Space, B. *Massively Parallel Monte Carlo (MPMC)*. 2012, Available on GitHub. <https://github.com/mpmccode/mpmc>.
13. Liu, J.; Fernandez, C. A.; Martin, P. F.; Thallapally, P. K.; Strachan, D. M. *Industrial & Engineering Chemistry Research* **2014**, *53*, 12893.

Reviewers' comments:

Reviewer #1 (Remarks to the Author):

The authors found that among the series of SIFSIX-3 MOFs, SIFSIX-3-Cu is good for <sup>85</sup>Kr removal from nuclear reprocessing plants because it is radioactively stable and can selectively separate and store <sup>85</sup>Kr using a two-bed breakthrough method. The topic is very interesting and the founding is attractive. However, their materials are already known ones and their results do not provide sufficient scientific insight.

Most of all, the authors did not provide any explanation why SIFSIX-3-Cu is more radioactively stable than the other SIFSIX-3-M materials. They should have provided suggestions or explanations for the reason by using proper calculations or further experimental characterizations.

Secondly, they argued that their materials have high Kr/N<sub>2</sub> selectivities than other benchmark adsorbents. But, they did not provide any comparison with other adsorbents. Moreover, I guess many other adsorbents can have good Kr/N<sub>2</sub> selectivities due to the differences in the polarizabilities of two molecules. It would have been more meaningful if the radioactive stability of SIFSIX-3-Cu was compared with other benchmark adsorbents.

For the above reasons, it is regrettable that I cannot recommend this paper to be published in a prestige journal like Nature Comm.

Reviewer #2 (Remarks to the Author):

This manuscript explores the possibility of using SIFSIX-based small pore MOFs for Kr separation from fission gas in the presence of Xe, CO<sub>2</sub>, N<sub>2</sub> and O<sub>2</sub>. The authors identified that SIFSIX-Cu is not only stable enough under radiation, but also has the ability of capture and separation of Kr from the UNF off-gas if a two-bed arrangement is used. The work is important and novel. The results are interesting. The paper is well written. I recommend it be accepted after the authors take care of the following.

It is not immediate clear from the main text if the PXRD patterns shown in Figure 2 are as-made or activated samples. But the SI indicates that the authors only examined as-made materials. I strongly believe that the authors should irradiate activated MOFs and investigate their stability as the phase behavior of as-made and activated MOFs can be very different. It is the activated MOFs that are used for adsorption. A recent paper (J. Phys. Chem. C 2019, 123, 17798–17807) shows that the metal environment in as-made and activated SIFSIX-Zn can be very different, which should be cited.

I was also wondering if they looked at those unknown phases to see if they still adsorb Kr.

Is there any evidence backing up the very last sentence of Results and Discussion section suggesting Kr adsorption is due to SiF<sub>6</sub><sup>2-</sup> pillars?

Reviewer #3 (Remarks to the Author):

Management of spent nuclear fuel is one of the important challenges in any nuclear industry because of high radio-toxicity associated with it. Various physico-chemical processes are framed for the extraction of valuable elements from nuclear wastes and containment of radioactive gases. However, all the chemicals or materials to be used for these processes must be radiation-resistant for them to work efficiently. Chosen chemicals or materials designed for extraction of valuable elements either through liquid-liquid extraction processes or trapping of various fission gasses by porous materials (e.g. Metal-organic frameworks) will not be of any use if the designed materials are not stable in presence of high radiation dose. Therefore, designing radiation-resistant efficient materials is very

important for management of nuclear wastes. Among various fission gases, managing radioactive xenon (Xe) and krypton (Kr) is a great challenge because of inert nature of the noble gases, Xe and Kr. The present communication deals with performance evaluation of a family of ultra-micro-porous metal-organic framework materials, SIFSIX-3-M (M = Fe, Co, Ni, Cu, Zn) for Kr removal from used nuclear fuel. Among all the materials considered in this work, SIFSIX-3-Cu has been found to be the most stable one when subjected to gamma radiation. The most important outcome of the present study is to selectively adsorb Kr gas in the second bed. In my opinion, the proposed radiation-resistant material, SIFSIX-3-Cu, for the purpose of selective adsorption of Xe and Kr seems to be quite efficient, which has been thoroughly investigated through various techniques including computational methods. The work presented in the manuscript is novel for two reasons: (1) selective adsorption of Kr and (2) Evaluation study of irradiation stability of MOF, and subsequent establishment of SIFSIX-3-Cu as a radiation-resistant MOF. It may be accepted for publication in Nature Communications after following points are addressed appropriately:

Is it possible to do two-bed breakthrough experiments with different loadings of noble gases (other than 400 ppm of Xe and 40 ppm of Kr), keeping the Xe/Kr ratio same? This study will provide new insights.

Irradiation induced phase change has been mentioned and the results are reported in the supplementary information for various radiation doses. One of the figures from the supplementary information (particularly the Figure S15 corresponding to 50 kGy, SIFSIX-3-Cu) may be moved to the main manuscript. The possibility of fragmentation through radiation degradation of a material cannot be ruled out; however, no such comment is made in the manuscript.

Grimme's D3 semiempirical method (available in VASP) is more accurate and should be used instead of D2 method. VASP version is not mentioned!

In the supplementary information: I fail to understand the phrase, "the Xe•••F distances for the annealed position were measured to be 1.94, 1.96, 1.98, and 2.00 Å, while distances of 2.14, 2.18, 2.22, and 2.25 Å were measured for the Kr•••F interaction." What do you want to convey with the shorter Xe---F distances? Also how Xe---F distance is shorter than the Kr---F distance?

It has been demonstrated that a combination of weak intermolecular interactions at low loadings and strong guest-guest interactions at high loadings leading to self-aggregation of guest molecules within confined space are responsible for adsorption of gasses in MFM-300 metal-organic frameworks. This confinement induced adsorption is a comparatively new strategy and related papers may be cited : . Zhang et al, "Confinement of Iodine Molecules into Triple-Helical Chains within Robust Metal-Organic Frameworks", J. Am. Chem. Soc. 2017, 139, 16289-16296; Srinivasu et al, "Confinement-Directed Adsorption of Noble Gases (Xe/Kr) in MFM-300(M)-Based Metal-Organic Framework Materials" J. Phys. Chem. C 2019, 123, 27531-27541.

## Reviewer #1:

*The authors found that among the series of SIFSIX-3 MOFs, SIFSIX-3-Cu is good for  $^{85}\text{Kr}$  removal from nuclear reprocessing plants because it is radioactively stable and can selectively separate and store  $^{85}\text{Kr}$  using a two-bed breakthrough method. The topic is very interesting and the founding is attractive. However, their materials are already known ones and their results do not provide sufficient scientific insight.*

*Most of all, the authors did not provide any explanation why SIFSIX-3-Cu is more radioactively stable than the other SIFSIX-3-M materials. They should have provided suggestions or explanations for the reason by using proper calculations or further experimental characterizations.*

Cu-N bonds are stronger than those of other M-N analogues. This is supported by shorter Cu-N bond distance of 1.9 Å in the SIFSIX-3-Cu compared to other M-N analogues (2.1 Å). The stronger Cu bonds lead to a more robust structure. Also, it was reported that the SIFSIX-3-Cu has a slightly smaller unit cell of 378 versus 388 Å<sup>3</sup> for SIFSIX-3-Zn, where the authors attributed this observation to the relatively stronger bonding between the Cu(II) and the pyrazine.

*Secondly, they argued that their materials have high Kr/N<sub>2</sub> selectivities than other benchmark adsorbents. But, they did not provide any comparison with other adsorbents. Moreover, I guess many other adsorbents can have good Kr/N<sub>2</sub> selectivities due to the differences in the polarizabilities of two molecules. It would have been more meaningful if the radioactive stability of SIFSIX-3-Cu was compared with other benchmark adsorbents.*

The choice of the right material for the  $^{85}\text{Kr}$  separation from nuclear reprocessing plants is based on several criteria: (1) Preferential adsorption of Xe and CO<sub>2</sub> over Kr so these two gases can be separated in the first bed, and (2) Preferential adsorption of Kr over N<sub>2</sub> and O<sub>2</sub> so the Kr can be adsorbed in the second bed in more pure form with minimum waste volume. If the material fulfills these two criteria, then it should be qualified for the radiation stability study. If the material does not achieve these two criteria, it is trivial to examine their radiation stability because they did not fulfill the main purpose of the Kr removal presented herein, which is the reduction of waste volume and Kr separation in more pure form with minimal amounts of other competing gases. The benchmark materials, SBMOF-1, Ni-MOF-74 and Ag mordenite, showed remarkable performance for Xe/Kr separation, however, they are not suitable for the  $^{85}\text{Kr}$  separation from spent fuel using the two-bed technique. Ni-MOF-74 and Ag mordenite were found to have poor Kr/N<sub>2</sub> selectivity, while, SBMOF-1<sup>24</sup> showed low Kr/CO<sub>2</sub> which prohibit the separation of the Kr in pure form.

Figure S21 in the SI demonstrated the low Kr/N<sub>2</sub> selectivity of the Ni-MOF-74. The separation data of Ag mordenite and SBMOF-1 are reported in the literature and the references are cited in the manuscript.

We thank the reviewer for this excellent suggestion to investigate the radiation stability of the benchmark materials. We are currently carrying out a more comprehensive study of the radiation stability of various materials, which will be included in a future paper.

*For the above reasons, it is regrettable that I cannot recommend this paper to be published in a prestige journal like Nature Comm.*

## **Reviewer #2:**

*This manuscript explores the possibility of using SIFSIX-based small pore MOFs for Kr separation from fission gas in the presence of Xe, CO<sub>2</sub>, N<sub>2</sub> and O<sub>2</sub>. The authors identified that SIFSIX-Cu is not only stable enough under radiation, but also has the ability of capture and separation of Kr from the UNF off-gas if a two-bed arrangement is used. The work is important and novel. The results are interesting. The paper is well written. I recommend it be accepted after the authors take care of the following.*

*It is not immediate clear from the main text if the PXRD patterns shown in Figure 2 are as-made or activated samples. But the SI indicates that the authors only examined as-made materials. I strongly believe that the authors should irradiate activated MOFs and investigate their stability as the phase behavior of as-made and activated MOFs can be very different. It is the activated MOFs that are used for adsorption. A recent paper (J. Phys. Chem. C 2019, 123, 17798–17807) shows that the metal environment in as-made and activated SIFSIX-Zn can be very different, which should be cited.*

The SIFSIX-3-Cu has the same radiation stability either at the as-synthesized form or the activated form. Further study of the stability of the material under Beta radiation was performed on the activated SIFSIX-3-Cu sample and the PXRD pattern was compared with the simulated pattern in Figure 2f.

*I was also wondering if they looked at those unknown phases to see if they still adsorb Kr.*

We believe any destruction or degradation of the SIFSIX-3-M materials will lead to non-porous structures from the crystallographic point of view since SIFSIX-3-M is a *pcu* network and has only one-dimensional channel. Even if only the M-F bond gets broken to go from 3D to 2D structure the SiF<sub>6</sub> pillar has to travel to the channel, which will block the pore especially the material has a very narrow pore of 3.6 Å.

*Is there any evidence backing up the very last sentence of Results and Discussion section suggesting Kr adsorption is due to SiF<sub>6</sub>-pillars?*

Figures 3(c) and S23 show that the modeled binding site for Kr in **SIFSIX-3-Cu** is between four neighboring  $\text{SiF}_6^{2-}$  pillars within the square grid.

Furthermore, we performed periodic density functional theory (DFT) calculations for Xe, Kr,  $\text{CO}_2$ ,  $\text{N}_2$ , and  $\text{O}_2$  within **SIFSIX-3-Cu** to determine the optimal binding site for these gases in the material and subsequently compute the adsorption energies ( $\Delta E$ ). The details for executing these calculations are now added to the “Modeling studies in SIFSIX-3-Cu” section in the SI. The optimized position for all adsorbates in the MOF was discovered to be between four adjacent  $\text{SiF}_6^{2-}$  pillars. Figures illustrating these have been added to the SI (now Figures S24-S28). In addition, the following sentence is now listed as the very last sentence of the “Results and Discussion” section of the manuscript:

“Indeed, modeling studies revealed that the adsorbate localizes between four neighboring  $\text{SiF}_6^{2-}$  pillars within the small pores in this class of materials.”

Additionally, we now provide the calculated  $\Delta E$  values for all adsorbates in **SIFSIX-3-Cu** in Table S1. The following trend can be observed in the MOF–adsorbate interaction strength on the basis of these values:  $\text{CO}_2 > \text{Xe} > \text{Kr} > \text{N}_2 > \text{O}_2$ . This is fully consistent with the trends in the gas uptakes within the experimental adsorption isotherms displayed in Figure 3(a). Moreover, these results support the experimental findings/conclusions that **SIFSIX-3-Cu** preferentially adsorb  $\text{CO}_2$  and Xe over Kr and Kr over  $\text{N}_2$  and  $\text{O}_2$ . The following sentence has been added to the end of the third paragraph of the “Results and Discussion” section of the manuscript to indicate that such calculations support the experimental results:

“Furthermore, periodic density functional theory (DFT) calculations confirm that SIFSIX-3-Cu is selective for  $\text{CO}_2$  and Xe over Kr and Kr over  $\text{N}_2$  and  $\text{O}_2$  on the basis of the calculated adsorption energies in the material (Table S1).”

### **Reviewer #3:**

*Management of spent nuclear fuel is one of the important challenges in any nuclear industry because of high radio-toxicity associated with it. Various physico-chemical processes are framed for the extraction of valuable elements from nuclear wastes and containment of radioactive gases. However, all the chemicals or materials to be used for these processes must be radiation-resistant for them to work efficiently. Chosen chemicals or materials designed for extraction of valuable elements either through liquid-liquid extraction processes or trapping of various fission gasses by porous materials (e.g. Metal-organic frameworks) will not be of any use if the designed materials are not stable in presence of high radiation dose. Therefore, designing radiation-resistant efficient materials is very important for management of nuclear wastes. Among various fission gases, managing radioactive xenon (Xe) and krypton (Kr) is a great challenge because of inert nature of the noble gases, Xe and Kr. The present communication deals with performance evaluation of a family of ultra-micro-porous metal-organic framework materials, SIFSIX-3-M (M = Fe, Co, Ni, Cu, Zn) for Kr removal from used nuclear fuel. Among all the materials considered in this work, SIFSIX-3-Cu has been found to be the most stable one*

*when subjected to gamma radiation. The most important outcome of the present study is to selectively adsorb Kr gas in the second bed. In my opinion, the proposed radiation-resistant material, SIFSIX-3-Cu, for the purpose of selective adsorption of Xe and Kr seems to be quite efficient, which has been thoroughly investigated through various techniques including computational methods. The work presented in the manuscript is novel for two reasons: (1) selective adsorption of Kr and (2) Evaluation study of irradiation stability of MOF, and subsequent establishment of SIFSIX-3-Cu as a radiation-resistant MOF. It may be accepted for publication in Nature Communications after following points are addressed appropriately:*

*Is it possible to do two-bed breakthrough experiments with different loadings of noble gases (other than 400 ppm of Xe and 40 ppm of Kr), keeping the Xe/Kr ratio same? This study will provide new insights.*

The choice of this composition is based on the actual composition of UNF off-gas. However, this is an insightful comment and will consider these measurements in future work.

We agree with reviewer, keeping noble gas concentration the same and varying other gas composition provide new insights but these experiments are beyond the scope of this work. However, we will follow up with another paper focused on reviewer suggestion and role of particle size and shape affect the noble gas selectivity.

*Irradiation induced phase change has been mentioned and the results are reported in the supplementary information for various radiation doses. One of the figures from the supplementary information (particularly the Figure S15 corresponding to 50 kGy, SIFSIX-3-Cu) may be moved to the main manuscript. The possibility of fragmentation through radiation degradation of a material cannot be ruled out; however, no such comment is made in the manuscript.*

Figure 2f was added to the manuscript that also demonstrated the stability of the SIFSIX-3-Cu under beta radiation and the suggested comment was discussed in the manuscript.

*Grimme's D3 semiempirical method (available in VASP) is more accurate and should be used instead of D2 method. VASP version is not mentioned!*

We optimized the unit cell of **SIFSIX-3-Cu** using the DFT-D3 method, but surprisingly found that the energy of the resulting crystal structure is higher than that obtained using the DFT-D2 method (−705.5814605 vs −706.2898731 eV). Because the DFT-D2 method resulted in a crystal structure that was lower in energy, we decided to use this structure for the classical simulations. This is now summarized within the second paragraph of the “Modeling studies in SIFSIX-3-Cu” section in the SI.

The version of VASP that was utilized is 5.4.4; this is now mentioned in the aforementioned section in the SI.

*In the supplementary information: I fail to understand the phrase, “the Xe•••F distances for the annealed position were measured to be 1.94, 1.96, 1.98, and 2.00 Å, while distances of 2.14, 2.18, 2.22, and 2.25 Å were measured for the Kr•••F interaction.” What do you want to convey with the shorter Xe---F distances ? Also how Xe---F distance is shorter than the Kr---F distance?*

If considering the distances between the center-of-mass (COM) of the equatorial F atoms and the COM of both Xe and Kr, then the measured distances would be nearly identical between the adsorbates. For the record, when measuring between the two COMs, the Xe•••F distances are 3.44, 3.46, 3.48, 3.50 Å, while those for Kr•••F are 3.44, 3.48, 3.52, and 3.55 Å. However, if these distances are subtracted by both the atomic radius of F (0.42 Å) and the atomic radius for the noble gas (Xe = 1.08 Å, Kr = 0.88 Å), then distances of 1.94, 1.96, 1.98, and 2.00 Å are obtained for the Xe•••F interaction, while distances of 2.14, 2.18, 2.22, and 2.25 Å are obtained for Kr•••F. Since Xe exhibits a larger atomic radius than Kr, the distance between the *surface* of the atom to that of an equatorial F atom is shorter than the corresponding distance for Kr•••F.

It is well-known in the MOF literature that shorter adsorbent–adsorbate distances corresponds to stronger interactions between the adsorbent and the adsorbate. By mentioning that the Xe•••F interaction distances are shorter than those for Kr•••F, we want to imply that the interaction between **SIFSIX-3-Cu** and Xe is stronger compared to that between the MOF and Kr. This is consistent with experimental findings that **SIFSIX-3-Cu** displays higher affinity toward Xe than Kr.

*It has been demonstrated that a combination of weak intermolecular interactions at low loadings and strong guest–guest interactions at high loadings leading to self-aggregation of guest molecules within confined space are responsible for adsorption of gasses in MFM-300 metal-organic frameworks. This confinement induced adsorption is a comparatively new strategy and related papers may be cited : . Zhang et al, “Confinement of Iodine Molecules into Triple-Helical Chains within Robust Metal–Organic Frameworks”, *J. Am. Chem. Soc.* 2017, 139, 16289-16296; Srinivasu et al, “Confinement-Directed Adsorption of Noble Gases (Xe/Kr) in MFM-300(M)-Based Metal–Organic Framework Materials” *J. Phys. Chem. C* 2019, 123, 27531-27541.*

The suggested paper “*J. Phys. Chem. C* 2019, 123, 27531-27541” is cited in the manuscript. Thanks for the suggestion.

Reviewers' comments:

Reviewer #1 (Remarks to the Author):

I still think that major issues raised by the reviewer have not been fully addressed. I recommend the publication if the following points are clearly addressed.

The authors attributed the observed radioactive stability of SIFSIX-3-Cu to the stronger Cu-N bonds than other M-N analogues by mentioning the shorter Cu-N bond distance (1.9 Å) than the other the M-N bond distances (2.1 Å). From the PXRD measurements after the gamma radiation at different intensities, the radioactive stabilities of SIFSIX-M show the following order: Cu > Co > Fe > Zn and Ni. Could this order be explained by the bond distances? The authors should clearly explain this.

The authors argued that they chose the right material for the 85Kr separation from nuclear reprocessing plants based on two criteria: (1) Preferential adsorption of Xe and CO<sub>2</sub> over Kr so these two gases can be separated in the first bed, and (2) Preferential adsorption of Kr over N<sub>2</sub> and O<sub>2</sub> so that Kr can be adsorbed in the second bed. However, I do not understand why the same adsorbent material should be used for both beds. I think two different adsorbent materials can be used for each bed. Since SBMOF-1, Ni-MOF-74 and Ag mordenite showed remarkable performance for Xe/Kr separation, these materials can be used for the first bed. Therefore, it would be more meaningful if the radioactive stability of these benchmark adsorbents are also compared.

Although the authors cited the references including the Kr/N<sub>2</sub> separation data of Ag mordenite and SBMOF-1, these should be shown in the supporting information for the comparisons.

I found the following paper: "Adsorptive separation of xenon/krypton mixtures using a zirconium-based metal-organic framework with high hydrothermal and radioactive stabilities, Journal of Hazardous Materials 320 (2016) 513–520." This paper also studied radioactive stability of a zirconium-based MOF for Xe/Kr separation. I guess the authors may have not noticed this paper. It should be properly referenced.

Page 8, line 165: "SBMOF-1 showed low Kr/CO<sub>2</sub> which prohibit the separation of the Kr in pure form."  
--> Is low Kr/CO<sub>2</sub> correct? It could be low Kr/O<sub>2</sub>.

Reviewer #2 (Remarks to the Author):

The authors addressed most of the issues raised by three reviewers reasonably well. Thus, I am supportive of acceptance. However, both reviewers 2 and 3 suggested several references to be included and it is disappointing to see only one was cited. I hope they will all be included in the final version.

Reviewer #3 (Remarks to the Author):

Authors have suitably revised the manuscript. By and large all the comments are addressed successfully. I recommend the manuscript to be accepted as is.

*Reviewers' comments:*

*Reviewer #1 (Remarks to the Author):*

*I still think that major issues raised by the reviewer have not been fully addressed. I recommend the publication if the following points are clearly addressed.*

*The authors attributed the observed radioactive stability of SIFSIX-3-Cu to the stronger Cu-N bonds than other M-N analogues by mentioning the shorter Cu-N bond distance (1.9 Å) than the other the M-N bond distances (2.1 Å). From the PXRD measurements after the gamma radiation at different intensities, the radioactive stabilities of SIFSIX-M show the following order: Cu > Co > Fe > Zn and Ni. Could this order be explained by the bond distances? The authors should clearly explain this.*

We thank the reviewer for highlighting this point. We are aware that more in-depth study is required to better understand the mechanism of radiation absorption by the framework. This will be part of our future studies as it depends on many factors and it is out of the scope of the current work. The scope of the paper is more toward application more than theoretical investigation. There are only few reported studies for radiation stability of MOFs and we believe more studies need to be done at this area. For example, we tried to use the NIST XCOM: Photon Cross Sections Database which is mainly looking to the metal center as the main factor for stability. However, the results did not support our data, presumably, because there are many factors that can contribute to the radiation stability not only the metal centers since MOFs are composed of metal, organic and/or inorganic linkers with M-O/M-N/M-F bonds. We believe that the radiation stability of the MOF framework can depend on many factors such as chemical bond strength, understanding which part of the framework absorbs the energy and where this energy goes. We think better model need to be created and more careful calculation is needed

Therefore, we believe that the current explanation of the shorter Cu-N bond distance compared to the other analogues is enough at this stage to elucidate why the SIFSIX-3-Cu is the more radiation-stable material and thereby the best analogue for the application presented herein. SIFSIX-3-Cu has shorter M-N bond of 1.9 Å compared to other analogues which show very small differences in M-N bond distance. According to CCDC, Cu tends to bond with N donor ligand more readily compared to Co, Fe, Zn and Ni. Therefore, bond strength could be the main factor behind the stability of SIFSIX-Cu framework which reaches up to 50 kGy, while other materials demonstrate much lower stability that reaches to only 10 kGy in case of Co. The bond distance in the other analogues are around the same  $2.15 \pm 0.04$  Å. We believe there are other factors controlling the stability of the other analogues and we are currently working on making a model to better understand the radiation absorption by the framework.

*The authors argued that they chose the right material for the <sup>85</sup>Kr separation from nuclear reprocessing plants based on two criteria: (1) Preferential adsorption of Xe and CO<sub>2</sub> over Kr so these two gases can be separated in the first bed, and (2) Preferential adsorption of Kr over N<sub>2</sub> and O<sub>2</sub> so that Kr can be adsorbed in the second bed. However, I do not understand why the*

*same adsorbent material should be used for both beds. I think two different adsorbent materials can be used for each bed. Since SBMOF-1, Ni-MOF-74 and Ag mordenite showed remarkable performance for Xe/Kr separation, these materials can be used for the first bed. Therefore, it would be more meaningful if the radioactive stability of these benchmark adsorbents are also compared.*

We are currently working on the radiation stability of several MOFs including the aforementioned MOFs by the reviewer and theoretical study on the mechanism of radiation absorption by the MOF structure. This data will be included in a follow-up paper.

*Although the authors cited the references including the Kr/N<sub>2</sub> separation data of Ag mordenite and SBMOF-1, these should be shown in the supporting information for the comparisons.*

The data for the SBMOF-1 and Ag mordenite were added in **Figure S22** and **Figure S30** in the SI.

*I found the following paper: “Adsorptive separation of xenon/krypton mixtures using a zirconium-based metal-organic framework with high hydrothermal and radioactive stabilities, Journal of Hazardous Materials 320 (2016) 513–520.” This paper also studied radioactive stability of a zirconium-based MOF for Xe/Kr separation. I guess the authors may have not noticed this paper. It should be properly referenced.*

The paper is properly discussed and cited in the main manuscript (**Page 3**).

*Page 8, line 165: “SBMOF-1 showed low Kr/CO<sub>2</sub> which prohibit the separation of the Kr in pure form.” --> Is low Kr/CO<sub>2</sub> correct? It could be low Kr/O<sub>2</sub>.*

This is not a mistake. As shown in **Figure S22** in the SI, SBMOF-1 shows very low Kr/CO<sub>2</sub> selectivity which means that the CO<sub>2</sub> cannot be separated from Kr.

*Reviewer #2 (Remarks to the Author):*

*The authors addressed most of the issues raised by three reviewers reasonably well. Thus, I am supportive of acceptance. However, both reviewers 2 and 3 suggested several references to be included and it is disappointing to see only one was cited. I hope they will all be included in the final version.*

All the references suggested by reviewers have been cited. Thank you for your kind review of our manuscript.

*Reviewer #3 (Remarks to the Author):*

*Authors have suitably revised the manuscript. By and large all the comments are addressed successfully. I recommend the manuscript to be accepted as is.*

Thank you for your kind recommendation that our work be accepted to Nature Communications.

REVIEWERS' COMMENTS:

Reviewer #1 (Remarks to the Author):

Although some issues related to the mechanism of radiation absorption have not been fully addressed, I think it is now publishable since most of the comments from the reviewers have been answered and revised.